AIMS Mathematics, 10(6): 14434–14458.
DOI: 10.3934/math.2025649
Received: 12 December 2024
Revised: 29 January 2025
Accepted: 13 February 2025
Published: 23 June 2025

https://www.aimspress.com/journal/Math

Research article

Diversity of the soliton solutions and sensitivity analysis for a fractional stochastic dynamical system: Applications to certain ferromagnetic materials

Badr Saad T. Alkahtani*

Department of Mathematics, College of Science, King Saud University, Riyadh 11989, Saudi Arabia

* **Correspondence:** Email: balqahtani1@ksu.edu.sa.

Abstract: In this article, we methodically investigate the fractional stochastic Kraenkel–Manna–Merle system (KMMS), which explains how a magnetic field propagates in a ferromagnet with zero conductivity and may shed light on a number of intriguing scientific occurrences. A suitable wave transformation is used to convert the governing equation into an ordinary differential equation (ODE). We thoroughly evaluate the innovative soliton solutions in the forms of dark, bright–dark, dark–bright, periodic, singular, hyperbolic, mixed trigonometric, and rational forms using the improved $\mathscr{F}$-expansion approach and the new extended direct algebraic method (NEDAM). Furthermore, a sensitivity analysis is carried out to investigate the impact of different factors on the behavior of the system. In order to shed light on the model's physical behavior, the study displays graphical plots of the chosen solutions using the selected methodologies. These techniques offer a strong foundation for resolving nonlinear fractional differential equations, which are crucial for simulating intricate ferromagnetistic physical processes. The resulting solutions demonstrate the fractional stochastic KMMS's complex structures and dynamic behavior.

Keywords: fractional stochastic KMMS; stochastic soliton solution; NEDAM; improved $\mathscr{F}$-expansion scheme; sensitivity analysis
Mathematics Subject Classification: 35C08, 60H15

1. Introduction

The ability of nonlinear partial differential equations (NLPDEs) to simulate complicated events makes them essential in many scientific and engineering domains [1–4]. A wide range of real-world phenomena, such as fluid dynamics [5], electromagnetic fields [6], quantum physics [7], chemical reactions [8], biological processes [9], and financial markets [10] need the proper modeling of NLPDEs. NLPDEs are known to be very nonlinear and complicated, having considerable science and

engineering challenges [11]. They have frequently called for some sophisticated methods of analysis and solutions, helping the creation of novel mathematical theories and procedures [12]. It is certain that future advances in our comprehension and management of the intricacies of the natural and technological worlds will be facilitated by the ongoing development of techniques for solving and analyzing NLPDEs. A crucial and quickly expanding area of mathematics, fractional calculus (FC), has important applications in science, engineering, and other fields. A more precise and thorough framework for comprehending complex systems is provided by its capacity to describe memory, hereditary characteristics, and nonlocal impacts. The multidisciplinary uses of FC highlight its significance in stimulating creativity and expanding knowledge in a range of fields. Numerous disciplines, including physics, engineering, biology, finance, environmental science, and more, have used them [13]. Fractional calculus improves the understanding, prediction, and management of complex phenomena in a variety of scientific and technical disciplines by offering more precise and thorough models.

On the other hand, stochastic partial differential equations (SPDEs) are a variant of partial differential equations (PDEs) that use stochasticity to model systems impacted by uncertainty and noise. SPDEs are employed in fields including economics, physics, biology, and engineering, where random effects are significant [14]. A significant amount of research on ferromagnetic materials has become publicly available in recent decades because of the rapid advancements in information technology and the demand for large amounts of data and high-density storage. Recent developments in technology have made it possible to make tiny ferromagnetic particles. Understanding the properties of microstructures and super microstructures in nanoscale ferrous metals is essential. If all the nanoparticles in the population are roughly the same size, then the magnetization of the population can be theoretically described by a magnetic moment. Ferromagnetic particles have magnetic moments that travel in opposite directions, enabling information to be shared between them. Solitons are always produced by these interactions. Consequently, a wide range of phenomena associated with the propagation of solitary waves have been examined. Numerous effective techniques have been used to solve NLPDEs. These techniques include the following: The modified Jacobi elliptic expansion method [15], the Riccita projective equation method [16], the scattering method [17], Hirota's bilinear method [18], the tanhcoth method [19], the variational iteration method [20], and numerous others [21]. Researchers have used these approaches, each offering unique benefits, to address the difficulties associated with NLPDEs in a number of scientific domains.

A complex mathematical model that describes the complex behaviors of ferromagnetic materials under the influence of stochastic (random) forces and memory effects is the fractional stochastic Kraenkel–Manna–Merle (KMM) system [22]. A sophisticated mathematical model known as the fractional stochastic Kraenkel–Manna–Merle (KMM) system captures the complicated behaviors of ferromagnetic materials under the impact of stochastic (random) forces and memory effects [23]. This system captures the memory effects, hereditary features, and random impacts typical of real-world ferromagnetic materials by merging stochastic processes with fractional calculus. Its significance extends to computational developments, theoretical studies, and real-world uses in a number of high-tech fields, such as magnetic sensing, spintronics, and magnetic storage [24]. Understanding this system improves our capacity to create, regulate, and optimize systems that use ferromagnetic materials, spurring advancement across a wide range of industries. In this research, we consider the

fractional stochastic Kraenkel–Manna–Merle system (FSKMMS) [25, 26]:

$$\begin{cases} \mathscr{D}_x^\beta \Theta_t - \Theta \mathscr{D}_x^\beta \phi + \sigma \mathscr{D}_x^\beta \phi = \kappa \mathscr{D}_x^\beta \Theta \mathbb{B}_t, \\ \mathscr{D}_x^\beta \phi_t - \Theta \mathscr{D}_x^\beta \Theta = \kappa \mathscr{D}_x^\beta \phi \mathbb{B}_t, \end{cases} \tag{1.1}$$

where $\mathscr{D}_x^\beta$ is the conformable derivative operator for $\beta \in (0, 1]$, σ denotes the damping coefficient, κ is the noise intensity, $\mathbb{B}$ is the Brownian motion (BM) [27], and $\mathbb{B} = \frac{\partial \mathbb{B}}{\partial t}$ represents the relationship between the magnetization, denoted by $\phi = \phi(x, t)$, and the external magnetic fields, represented by $\Theta = \Theta(x, t)$, with respect to the ferrite.

By setting $\beta = 1$ and $\kappa = 0$, we can construct the Kraenkel–Manna–Merle system (KMMS) as follows:

$$\begin{cases} \Theta_{xt} - \Theta \phi_x + \sigma \phi_x = 0, \\ \phi_{xt} - \Theta \Theta_x = 0. \end{cases} \tag{1.2}$$

This could explain how short waves propagate in saturated ferromagnetic materials in a nonlinear, zero-conductivity manner. Many scholars have recently developed analytical solutions to Eq (1.2), with ($\sigma = 0$). Li and Ma [28, 29], for instance, investigated the soliton solutions of the governing model using the $\frac{G'}{G}$-expansion method and auxiliary equation methods. Using the inverse scattering method, Tchokouansi et al. [30] obtained several traveling wave solutions for the governing model. Using the bilinear technique, Nguepjouo et al. [31] also extracted some optical solutions of the studied model and so on.

This paper aims to determine the stochastic solutions of the FSKMMS (1.1), using the improved $\mathscr{F}$-expansion method and NEDAM, two recently developed methodologies. Physicists would find the solutions offered to be extremely helpful in describing important physical processes. A sensitivity analysis is also carried out to investigate the impact of different factors on the behavior of the system. Additionally, we offer numerous graphical depictions utilizing Mathematica software to examine the impact of the fractional derivative on the precise resolution of the FSKMMS (1.1). The study helps us better understand the complex behaviors shown by the system. In light of the findings, it may be said that the study's motivation is that the data are novel, fascinating, and potentially very important in helping us understand how the FSKMMS behaves.

The structure of this article is as follows: In Section 2, we propose the definition and characteristics of the above mentioned derivative. In Section 3, we discuss the brief description of our methodologies. Section 4 demonstrates the implementation of the selected approaches. In Section 5, we examined the system's sensitivity analysis. The model's results and discussion are illustrated in Section 6. Finally, in Section 7, we outline our last point.

2. Conformable derivative

The conformable derivative (CD) [32], with its simplicity, intuitiveness, and preservation of basic features, is a major breakthrough in the field of FC. Its usefulness in modeling complex systems with fractional dynamics makes it an invaluable tool for a wide range of scientific and engineering fields, both in theoretical research and real-world applications.

In the following, we define some of the main characteristics of the conformable fractional derivative and talk about it.

Definition 2.1. For $\beta \in (0, 1]$, the CD of $\mathfrak{u} : \mathscr{R}^+ \to \mathscr{R}$ is defined as

$$\mathscr{D}_x^\beta \mathfrak{u}(z) = \lim_{\epsilon \to 0} \frac{\mathfrak{u}(x + \epsilon x^{1-\beta}) - \mathfrak{u}(x)}{\epsilon}. \tag{2.1}$$

If we suppose that $\mathfrak{u}$, $\phi : \mathscr{R}^+ \to \mathscr{R}$ are differentiable functions, then the CD has the following corollaries:

$$\begin{aligned}
\mathscr{D}_x^\beta[h_1\mathfrak{u}(z) + h_2\phi(z)] &= h_1\mathscr{D}_x^\beta \mathfrak{u}(z) + h_2\mathscr{D}_x^\beta \phi(z),\\
\mathscr{D}_x^\beta[h_1] &= 0, \text{ where } h_1 \text{ is a constant},\\
\mathscr{D}_x^\beta(\mathfrak{u}o\phi)(x) &= z^{1-\beta}\phi''(x)\mathfrak{u}(\phi(x)),\\
\mathscr{D}_x^\beta[x^n] &= nx^{n-\beta},\\
\mathscr{D}_x^\beta \mathfrak{u}(x) &= x^{1-\beta}\frac{d\mathfrak{u}}{dx},
\end{aligned}$$

for any real constants $h_1,\ h_2$. Moreover, the BM $\mathbb{B}$ is defined as follows:

Definition 2.2. Being stochastic, the BM $\mathbb{B}(\theta)_\theta \geq 0$ satisfies the following requirements:

$$\begin{aligned}
\mathbb{B} &= 0,\\
\mathbb{B} &\text{ is continuous if } t \geq 0,\\
\mathbb{B}(t_2) - \mathbb{B}(t_1) &\text{ is independent if } t_2 > t_1,\\
\mathbb{B}(t_2) - \mathbb{B}(t_1) &\text{ has a normal distribution } \mathscr{N}(0, t_2 - t_1).
\end{aligned}$$

We also define the following lemma.

Lemma 2.1. $\mathbb{E}(e^{\lambda\mathbb{B}(t)}) = e^{\frac{1}{2}\lambda^2 t}$ for $\lambda > 0$.

Brownian motion is fundamental to the applied and theoretical sciences. Its research crosses fields, offering insights into stochastic dynamics, unpredictability, and diffusion with practical applications in everything from financial markets to molecular biology.

3. Description of selected methodologies

Consider the fractional stochastic NLPDE of the following form:

$$\mathscr{J}(\mathscr{V}, D_t^\alpha \mathscr{V}, D_x^\beta \mathscr{V}, D_t^{2\beta}\mathscr{V}, D_x^{2\beta}\mathscr{V}, \nabla^\beta \mathscr{V}, \cdots) = \mathscr{F}(\mathscr{V}, t, x) + \mathscr{G}(\mathscr{V}, t, x)\mathbb{B}(t, x),\ 0 < \beta \leq 1, \tag{3.1}$$

where $\mathscr{V}(x, t)$ represents the unknown function; $\mathscr{F}(\mathscr{V}, t, x)$ represents a deterministic source or forcing term; $\mathscr{G}(\mathscr{V}, t, x)$ represents the noise intensity or diffusion coefficient, which may depend on the solution $\mathscr{V}$, time t, and space x; and $\mathbb{B}(t, x)$ represents a space time fractional noise, which can include Gaussian white noise. We apply the following wave transformation:

$$\mathscr{V}(x, t) = \psi(\eta)e^{(\kappa\mathbb{B}(t) - \frac{1}{2}\kappa^2 t)},\ \text{where } \eta = \frac{1}{\beta}\,\alpha\, x^\beta + \delta t. \tag{3.2}$$

Putting (3.2) into (3.1), we convert Eq (3.2) into an ODE.

$$\mathscr{P}(\psi, \psi', \psi'', \psi''', \cdots) = 0. \tag{3.3}$$

3.1. The NEDAM

Through the development and use of novel tools and approaches, the NEDAM [33] advances mathematical research in the subject of nonlinear dynamics and deepens our understanding of nonlinear systems and their behaviors.

Step 1. Assume the general solution of Eq (3.3) is presumed to be:

$$\psi(\eta) = \sum_{i=1}^{n} [\aleph_i \mathscr{H}(\xi)^i], \tag{3.4}$$

where $\aleph_i (i = 0,\ 1,\ 2, \cdots, n)$ is obtained later. From Eq (3.4), the function $\mathscr{H}(\eta)$ is satisfied by:

$$(\mathscr{H}'(\eta)) = Ln(a)(\vartheta_1 + \vartheta_2 \mathscr{H}(\eta) + \vartheta_3 (\mathscr{H}(\eta)^2),\ a \neq 0, 1, \tag{3.5}$$

where $\vartheta_i,\ i = 1, 2, 3$ are real constants.

Step 2. We apply balancing theory between the highest derivative and the power of the nonlinear term in Eq (3.3) to determine the value of n.

Step 3. By substituting Eqs (3.4) and (3.5) into Eq (3.3), an algebraic equation with a power of $\mathscr{H}(\eta)$ may be created. This equation can then be solved with Mathematica to produce the solution of Eq (3.6).

3.2. The improved $\mathscr{F}$-expansion scheme

The improved $\mathscr{F}$-expansion approach is a valuable tool in the study and practical application of NLPDEs because of its ability to generate precise solutions, streamline challenging issues, and broaden our comprehension of nonlinear systems. Its versatility, efficacy, and contribution to theoretical and practical features make it an essential method in modern scientific and technical research.

Step 1. Assume the general solution of Eq (3.6) to be as follows:

$$\psi(\eta) = \sum_{i=0}^{n} \lambda_i (\mathscr{M} + \mathscr{F}(\eta))^i + \sum_{i=1}^{n} \mu_i (\mathscr{M} + \mathscr{F}(\eta))^{-i}, \tag{3.6}$$

where λ_i and μ_i may not be zero at the same time. The function $\mathscr{F}$ is a solution of the ODE:

$$\mathscr{F}'(\eta) = \mathscr{Q} + \mathscr{F}^2(\eta). \tag{3.7}$$

The three general solutions of the Riccati equation (3.7) are as follows:

Case I: If $\mathscr{Q} < 0$, then

$$\mathscr{F}_1 = -\sqrt{-\mathscr{Q}} \tanh(\sqrt{-\mathscr{Q}}\eta), \tag{3.8}$$

$$\mathscr{F}_2 = -\sqrt{-\mathscr{Q}} \coth(\sqrt{-\mathscr{Q}}\eta). \tag{3.9}$$

Case II: If $\mathscr{Q} > 0$, then

$$\mathscr{F}_3 = \sqrt{\mathscr{Q}} \tan(\sqrt{\mathscr{Q}}\eta), \tag{3.10}$$

$$\mathscr{F}_4 = -\sqrt{\mathscr{Q}} \cot(\sqrt{\mathscr{Q}}\eta). \tag{3.11}$$

Case III: If $\mathscr{Q} = 0$, then

$$\mathscr{F}_5 = -\frac{1}{\eta}. \tag{3.12}$$

Step 2. We apply balancing theory between the highest derivative and the power of the nonlinear term to determine the value of n.
Step 3. Equations (3.7) and (3.8) can be substituted in Eq (3.6) to generate an algebraic equation with a power of $\mathscr{F}(\eta)$ that can be solved using Mathematica to provide the values of λ_i and μ_i.

4. Extraction of analytical solutions

The primary objective of this part is to get a variety of responses for the provided model. To obtain the soliton solutions of Eq (1.1), we propose the following wave transformation:

$$\Theta(x,t) = \varsigma(\eta)e^{(\kappa\mathbb{B}(t)-\frac{1}{2}\kappa^2 t)},\ \phi(x,t) = \vartheta(\eta)e^{(\kappa\mathbb{B}(t)-\frac{1}{2}\kappa^2 t)} \text{ where } \eta = \frac{1}{\beta}\,\alpha\, x^{\beta} + \delta t, \tag{4.1}$$

where α and δ are nonzero constants, $\varsigma(\eta)$ and $\vartheta(\eta)$ are real functions, and we are able to obtain the FSKMMS wave equation (1.1).

$$\mathscr{D}_x^{\beta}\Theta = \alpha\varsigma' e^{(\kappa\mathbb{B}(t)-\frac{1}{2}\kappa^2 t)}, \tag{4.2}$$

and

$$\begin{aligned}\mathscr{D}_x^{\beta}\Theta_t &= \alpha\delta\varsigma'' + \frac{1}{2}\alpha\kappa^2\varsigma' + \kappa\alpha\varsigma'\mathbb{B}_t - \frac{1}{2}\alpha\kappa^2\varsigma']e^{(\kappa\mathbb{B}(t)-\frac{1}{2}\kappa^2 t)}\\ &= [\alpha\delta\varsigma'' + \kappa\alpha\varsigma'\mathbb{B}_t]e^{(\kappa\mathbb{B}(t)-\frac{1}{2}\kappa^2 t)}.\end{aligned} \tag{4.3}$$

$$\mathscr{D}_x^{\beta}\phi = \alpha\vartheta' e^{(\kappa\mathbb{B}(t)-\frac{1}{2}\kappa^2 t)},\ \mathscr{D}_x^{\beta}\phi_t = [\alpha\delta\vartheta'' + \kappa\alpha\vartheta'\mathbb{B}_t]e^{(\kappa\mathbb{B}(t)-\frac{1}{2}\kappa^2 t)}. \tag{4.4}$$

Switching Eq (4.1) in Eq (1.1), we utilize

$$\begin{cases}\alpha\delta\varsigma'' - \alpha\varsigma\vartheta' e^{(\kappa\mathbb{B}(t)-\frac{1}{2}\kappa^2 t)} = 0,\\ \alpha\delta\vartheta'' - \alpha\varsigma\varsigma' e^{(\kappa\mathbb{B}(t)-\frac{1}{2}\kappa^2 t)} = 0.\end{cases} \tag{4.5}$$

Using the above mentioned lemma, where $\mathbb{B}(t)$ is a normal process with $\mathbb{E}(e^{\kappa\mathbb{B}(t)})$, Eq (4.5) becomes

$$\begin{cases}\delta\varsigma'' - \varsigma\vartheta' = 0\\ \delta\vartheta'' - \varsigma\varsigma' = 0.\end{cases} \tag{4.6}$$

By integrating Eq (4.6), we get

$$\vartheta' = \frac{1}{2\delta}\varsigma^2 + \frac{c}{\delta}. \tag{4.7}$$

Switching Eq (4.7) into the first equation in (4.6), we achieve

$$\varsigma'' - \frac{1}{2\delta^2}\varsigma^3 - \frac{c}{2\delta^2}\varsigma = 0. \tag{4.8}$$

4.1. Implementation of the NEDAM

Applying the balancing principle between the highest derivative ς'' and the largest power nonlinear term ς^3 yields $N = 1$ in Eq (4.8). Therefore, the nontrivial solution of Eq (4.8) becomes:

$$\varsigma(\eta) = \aleph_0 + \aleph_1 \mathscr{H}(\eta). \tag{4.9}$$

When (4.9) and its derivatives in (4.8) are combined, an algebraic system of equations with similar powers of $\varsigma(\eta)$ is produced. By solving them, we can ascertain the following sets of solutions:
Family 1:

$$\left\{\aleph_0 \to -\frac{\sqrt{2}\sqrt{c}\vartheta_2 \mathrm{Ln}(a)}{\sqrt{\left(\vartheta_2^2-4\vartheta_1\vartheta_3\right)\left(-\mathrm{Ln}(a)^2\right)}},\ \aleph_1 \to -\frac{2\sqrt{2}\sqrt{c}\vartheta_3 \mathrm{Ln}(a)}{\sqrt{\left(\vartheta_2^2-4\vartheta_1\vartheta_3\right)\left(-\mathrm{Ln}(a)^2\right)}},\ \delta \to \frac{\sqrt{2}\sqrt{c}}{\sqrt{\left(\vartheta_2^2-4\vartheta_1\vartheta_3\right)\left(-\mathrm{Ln}(a)^2\right)}}\right. . \tag{4.10}$$

Family 2:

$$\left\{\aleph_1 \to \frac{2\vartheta_3\aleph_0}{\vartheta_2},\ c \to \frac{1}{2}\left(\frac{4\vartheta_1\vartheta_3}{\vartheta_2^2}-1\right)\aleph_0^2,\ \delta \to -\frac{\aleph_0}{\vartheta_2 \mathrm{Ln}(a)}\right. . \tag{4.11}$$

Family 3:

$$\left\{\aleph_0 \to \vartheta_2\delta \mathrm{Ln}(a),\ \aleph_1 \to 2\vartheta_3\delta \mathrm{Ln}(a),\ c \to -\frac{1}{2}\left(\vartheta_2^2-4\vartheta_1\vartheta_3\right)\delta^2 \mathrm{Ln}(a)^2\right. . \tag{4.12}$$

Using Eq (1.1), we determined the following solutions for Family 1.
(1) For $\mathscr{G} = \vartheta_2^2 - 4\vartheta_1\vartheta_3 < 0$, and $\vartheta_3 \neq 0$.

• The trigonometric solutions:

Cluster 1:

$$\Theta_1(x,t) = \left[-\frac{\sqrt{2}\sqrt{c}\sqrt{-\mathscr{G}}\mathrm{Ln}(a)\mathrm{Tan}_a\left(\frac{\sqrt{-\mathscr{G}}\eta}{2}\right)}{\sqrt{\left(\vartheta_2^2-4\vartheta_1\vartheta_3\right)\left(-\mathrm{Ln}(a)^2\right)}}\right] e^{(\kappa\mathbb{B}(t)-\frac{1}{2}\kappa^2 t)}. \tag{4.13}$$

$$\phi_1(x,t) = \int\left[\frac{1}{2\delta}\left(-\frac{\sqrt{2}\sqrt{c}\sqrt{-\mathscr{G}}\mathrm{Ln}(a)\mathrm{Tan}_a\left(\frac{\sqrt{-\mathscr{G}}\eta}{2}\right)}{\sqrt{\left(\vartheta_2^2-4\vartheta_1\vartheta_3\right)\left(-\mathrm{Ln}(a)^2\right)}}\right)^2+\frac{c}{\delta}\right] e^{(\kappa\mathbb{B}(t)-\frac{1}{2}\kappa^2 t)}. \tag{4.14}$$

Cluster 2:

$$\Theta_2(x,t) = \left[\frac{\sqrt{2}\sqrt{c}\sqrt{-\mathscr{G}}\mathrm{Ln}(a)\mathrm{Cot}_a\left(\frac{\sqrt{-\mathscr{G}}\eta}{2}\right)}{\sqrt{\left(\vartheta_2^2-4\vartheta_1\vartheta_3\right)\left(-\mathrm{Ln}(a)^2\right)}}\right] e^{(\kappa\mathbb{B}(t)-\frac{1}{2}\kappa^2 t)}. \tag{4.15}$$

$$\phi_2(x,t) = \int\left[\frac{1}{2\delta}\left(\frac{\sqrt{2}\sqrt{c}\sqrt{-\mathscr{G}}\mathrm{Ln}(a)\mathrm{Cot}_a\left(\frac{\sqrt{-\mathscr{G}}\eta}{2}\right)}{\sqrt{\left(\vartheta_2^2-4\vartheta_1\vartheta_3\right)\left(-\mathrm{Ln}(a)^2\right)}}\right)^2+\frac{c}{\delta}\right] e^{(\kappa\mathbb{B}(t)-\frac{1}{2}\kappa^2 t)}. \tag{4.16}$$

• The combo-trigonometric solutions:

Cluster 3:

$$\Theta_3(x,t)=\Big[\frac{\sqrt{2}\,\sqrt{c}\,\sqrt{-\mathscr{G}}\mathrm{Ln}(a)\Big(\sqrt{mn}\mathrm{Sec}_a\Big(\sqrt{-\mathscr{G}}\eta\Big)+\mathrm{Tan}_a\Big(\sqrt{-\mathscr{G}}\eta\Big)\Big)}{\sqrt{\Big(\vartheta_2^2-4\vartheta_1\vartheta_3\Big)(-\mathrm{Ln}(a)^2)}}\Big]e^{(\kappa\mathbb{B}(t)-\frac{1}{2}\kappa^2 t)}. \quad (4.17)$$

$$\phi_3(x,t)=\int\Big[\frac{1}{2\delta}(\frac{\sqrt{2}\,\sqrt{c}\,\sqrt{-\mathscr{G}}\mathrm{Ln}(a)\Big(\sqrt{mn}\mathrm{Sec}_a\Big(\sqrt{-\mathscr{G}}\eta\Big)+\mathrm{Tan}_a\Big(\sqrt{-\mathscr{G}}\eta\Big)\Big)}{\sqrt{\Big(\vartheta_2^2-4\vartheta_1\vartheta_3\Big)(-\mathrm{Ln}(a)^2)}})^2+\frac{c}{\delta}\Big]e^{(\kappa\mathbb{B}(t)-\frac{1}{2}\kappa^2 t)}. \quad (4.18)$$

Cluster 4:

$$\Theta_4(x,t)=\Big[\frac{\sqrt{2}\,\sqrt{c}\,\sqrt{-\mathscr{G}}\mathrm{Ln}(a)\Big(\mathrm{Cot}_a\Big(\sqrt{-\mathscr{G}}\eta\Big)+\sqrt{mn}\mathrm{Csc}_a\Big(\sqrt{-\mathscr{G}}\eta\Big)\Big)}{\sqrt{\Big(\vartheta_2^2-4\vartheta_1\vartheta_3\Big)(-\mathrm{Ln}(a)^2)}}\Big]e^{(\kappa\mathbb{B}(t)-\frac{1}{2}\kappa^2 t)}. \quad (4.19)$$

$$\phi_4(x,t)=\int\Big[\frac{1}{2\delta}(\frac{\sqrt{2}\,\sqrt{c}\,\sqrt{-\mathscr{G}}\mathrm{Ln}(a)\Big(\mathrm{Cot}_a\Big(\sqrt{-\mathscr{G}}\eta\Big)+\sqrt{mn}\mathrm{Csc}_a\Big(\sqrt{-\mathscr{G}}\eta\Big)\Big)}{\sqrt{\Big(\vartheta_2^2-4\vartheta_1\vartheta_3\Big)(-\mathrm{Ln}(a)^2)}})^2+\frac{c}{\delta}\Big]e^{(\kappa\mathbb{B}(t)-\frac{1}{2}\kappa^2 t)}. \quad (4.20)$$

Cluster 5:

$$\Theta_5(x,t)=\Big[\frac{\sqrt{2}\,\sqrt{c}\,\sqrt{-\mathscr{G}}\mathrm{Ln}(a)\Big(\mathrm{Tan}_a\Big(\sqrt{-\mathscr{G}}\eta\Big)-\mathrm{Cot}_a\Big(\sqrt{-\mathscr{G}}\eta\Big)\Big)}{\sqrt{\Big(\vartheta_2^2-4\vartheta_1\vartheta_3\Big)(-\mathrm{Ln}(a)^2)}}\Big]e^{(\kappa\mathbb{B}(t)-\frac{1}{2}\kappa^2 t)}. \quad (4.21)$$

$$\phi_5(x,t)=\int\Big[\frac{1}{2\delta}(\frac{\sqrt{2}\,\sqrt{c}\,\sqrt{-\mathscr{G}}\mathrm{Ln}(a)\Big(\mathrm{Tan}_a\Big(\sqrt{-\mathscr{G}}\eta\Big)-\mathrm{Cot}_a\Big(\sqrt{-\mathscr{G}}\eta\Big)\Big)}{\sqrt{\Big(\vartheta_2^2-4\vartheta_1\vartheta_3\Big)(-\mathrm{Ln}(a)^2)}})^2+\frac{c}{\delta}\Big]e^{(\kappa\mathbb{B}(t)-\frac{1}{2}\kappa^2 t)}. \quad (4.22)$$

(2) For $\mathscr{G}=\vartheta_2^2-4\vartheta_1\vartheta_3>0$, and $\vartheta_3\neq 0$.

• The dark soliton solution

Cluster 6:

$$\Theta_6(x,t)=\Big[-\frac{\sqrt{2}\,\sqrt{c}\,\sqrt{\mathscr{G}}\mathrm{Ln}(a)\mathrm{Tanh}_a\Big(\frac{\sqrt{\mathscr{G}}\eta}{2}\Big)}{\sqrt{\Big(\vartheta_2^2-4\vartheta_1\vartheta_3\Big)(-\mathrm{Ln}(a)^2)}}\Big]e^{(\kappa\mathbb{B}(t)-\frac{1}{2}\kappa^2 t)}. \quad (4.23)$$

$$\phi_6(x,t)=\int\Big[\frac{1}{2\delta}(-\frac{\sqrt{2}\,\sqrt{c}\,\sqrt{\mathscr{G}}\mathrm{Ln}(a)\mathrm{Tanh}_a\Big(\frac{\sqrt{\mathscr{G}}\eta}{2}\Big)}{\sqrt{\Big(\vartheta_2^2-4\vartheta_1\vartheta_3\Big)(-\mathrm{Ln}(a)^2)}})^2+\frac{c}{\delta}\Big]e^{(\kappa\mathbb{B}(t)-\frac{1}{2}\kappa^2 t)}. \quad (4.24)$$

Cluster 7:

$$\Theta_7(x,t)=\Big[-\frac{\sqrt{2}\,\sqrt{c}\,\sqrt{\mathscr{G}}\mathrm{Ln}(a)\mathrm{Coth}_a\Big(\frac{\sqrt{\mathscr{G}}\eta}{2}\Big)}{\sqrt{\Big(\vartheta_2^2-4\vartheta_1\vartheta_3\Big)(-\mathrm{Ln}(a)^2)}}\Big]e^{(\kappa\mathbb{B}(t)-\frac{1}{2}\kappa^2 t)}. \quad (4.25)$$

$$\phi_7(x,t)=\int\Big[\frac{1}{2\delta}(-\frac{\sqrt{2}\,\sqrt{c}\,\sqrt{\mathscr{G}}\mathrm{Ln}(a)\mathrm{Coth}_a\left(\frac{\sqrt{\mathscr{G}}\eta}{2}\right)}{\sqrt{\left(\vartheta_2^2-4\vartheta_1\vartheta_3\right)(-\mathrm{Ln}(a)^2)}})^2+\frac{c}{\delta}\Big]e^{(\kappa\mathbb{B}(t)-\frac{1}{2}\kappa^2 t)}. \tag{4.26}$$

• The complex bright dark soliton solution

Cluster 8:

$$\Theta_8(x,t)=\Big[\frac{\sqrt{2}\,\sqrt{c}\,\sqrt{\mathscr{G}}\mathrm{Ln}(a)\left(-\mathrm{Tanh}_a\left(\sqrt{\mathscr{G}}\eta\right)+i\sqrt{mn}\mathrm{Sech}_a\left(\sqrt{\mathscr{G}}\eta\right)\right)}{\sqrt{\left(\vartheta_2^2-4\vartheta_1\vartheta_3\right)(-\mathrm{Ln}(a)^2)}}\Big]e^{(\kappa\mathbb{B}(t)-\frac{1}{2}\kappa^2 t)}. \tag{4.27}$$

$$\phi_8(x,t)=\int\Big[\frac{1}{2\delta}(\frac{\sqrt{2}\,\sqrt{c}\,\sqrt{\mathscr{G}}\mathrm{Ln}(a)\left(-\mathrm{Tanh}_a\left(\sqrt{\mathscr{G}}\eta\right)+i\sqrt{mn}\mathrm{Sech}_a\left(\sqrt{\mathscr{G}}\eta\right)\right)}{\sqrt{\left(\vartheta_2^2-4\vartheta_1\vartheta_3\right)(-\mathrm{Ln}(a)^2)}})^2+\frac{c}{\delta}\Big]e^{(\kappa\mathbb{B}(t)-\frac{1}{2}\kappa^2 t)}. \tag{4.28}$$

• The mixed singular soliton solution

Cluster 9:

$$\Theta_9(x,t)=\Big[\frac{\sqrt{2}\,\sqrt{c}\,\sqrt{\mathscr{G}}\mathrm{Ln}(a)\left(\sqrt{mn}\mathrm{Csch}_a\left(\sqrt{\mathscr{G}}\eta\right)-\mathrm{Coth}_a\left(\sqrt{\mathscr{G}}\eta\right)\right)}{\sqrt{\left(\vartheta_2^2-4\vartheta_1\vartheta_3\right)(-\mathrm{Ln}(a)^2)}}\Big]e^{(\kappa\mathbb{B}(t)-\frac{1}{2}\kappa^2 t)}. \tag{4.29}$$

$$\phi_9(x,t)=\int\Big[\frac{1}{2\delta}(\frac{\sqrt{2}\,\sqrt{c}\,\sqrt{\mathscr{G}}\mathrm{Ln}(a)\left(\sqrt{mn}\mathrm{Csch}_a\left(\sqrt{\mathscr{G}}\eta\right)-\mathrm{Coth}_a\left(\sqrt{\mathscr{G}}\eta\right)\right)}{\sqrt{\left(\vartheta_2^2-4\vartheta_1\vartheta_3\right)(-\mathrm{Ln}(a)^2)}})^2+\frac{c}{\delta}\Big]e^{(\kappa\mathbb{B}(t)-\frac{1}{2}\kappa^2 t)}. \tag{4.30}$$

• The dark singular soliton solution

Cluster 10:

$$\Theta_{10}(x,t)=\Big[-\frac{\sqrt{2}\,\sqrt{c}\,\sqrt{\mathscr{G}}\mathrm{Ln}(a)\left(\mathrm{Coth}_a\left(\frac{\sqrt{\mathscr{G}}\eta}{4}\right)+\mathrm{Tanh}_a\left(\frac{\sqrt{\mathscr{G}}\eta}{4}\right)\right)}{\sqrt{\left(\vartheta_2^2-4\vartheta_1\vartheta_3\right)(-\mathrm{Ln}(a)^2)}}\Big]e^{(\kappa\mathbb{B}(t)-\frac{1}{2}\kappa^2 t)}. \tag{4.31}$$

$$\phi_{10}(x,t)=\int\Big[\frac{1}{2\delta}(-\frac{\sqrt{2}\,\sqrt{c}\,\sqrt{\mathscr{G}}\mathrm{Ln}(a)\left(\mathrm{Coth}_a\left(\frac{\sqrt{\mathscr{G}}\eta}{4}\right)+\mathrm{Tanh}_a\left(\frac{\sqrt{\mathscr{G}}\eta}{4}\right)\right)}{\sqrt{\left(\vartheta_2^2-4\vartheta_1\vartheta_3\right)(-\mathrm{Ln}(a)^2)}})^2+\frac{c}{\delta}\Big]e^{(\kappa\mathbb{B}(t)-\frac{1}{2}\kappa^2 t)}. \tag{4.32}$$

(3) For $\vartheta_1\vartheta_3>0$ and $\vartheta_3=0$.

• The periodic soliton solutions

Cluster 11:

$$\Theta_{11}(x,t)=\Big[\frac{\sqrt{2}\,\sqrt{c}\mathrm{Ln}(a)\left(2\sqrt{\frac{\vartheta_1}{\vartheta_3}}\vartheta_3\mathrm{Tan}_a\left(\sqrt{\vartheta_1\vartheta_3}\eta\right)+\vartheta_2\right)}{\sqrt{\left(\vartheta_2^2-4\vartheta_1\vartheta_3\right)(-\mathrm{Ln}(a)^2)}}\Big]e^{(\kappa\mathbb{B}(t)-\frac{1}{2}\kappa^2 t)}. \tag{4.33}$$

$$\phi_{11}(x,t)=\int\Big[\frac{1}{2\delta}(\frac{\sqrt{2}\,\sqrt{c}\mathrm{Ln}(a)\left(2\sqrt{\frac{\vartheta_1}{\vartheta_3}}\vartheta_3\mathrm{Tan}_a\left(\sqrt{\vartheta_1\vartheta_3}\eta\right)+\vartheta_2\right)}{\sqrt{\left(\vartheta_2^2-4\vartheta_1\vartheta_3\right)(-\mathrm{Ln}(a)^2)}})^2+\frac{c}{\delta}\Big]e^{(\kappa\mathbb{B}(t)-\frac{1}{2}\kappa^2 t)}. \tag{4.34}$$

Cluster 12:

$$\Theta_{12}(x,t)=\Big[\frac{\sqrt{2}\,\sqrt{c}\mathrm{Ln}(a)\left(\vartheta_2-2\sqrt{\frac{\vartheta_1}{\vartheta_3}}\vartheta_3\mathrm{Cot}_a\left(\sqrt{\vartheta_1\vartheta_3}\eta\right)\right)}{\sqrt{\left(\vartheta_2^2-4\vartheta_1\vartheta_3\right)(-\mathrm{Ln}(a)^2)}}\Big]e^{(\kappa\mathbb{B}(t)-\frac{1}{2}\kappa^2 t)}. \tag{4.35}$$

$$\phi_{12}(x,t)=\int\Big[\frac{1}{2\delta}(\frac{\sqrt{2}\,\sqrt{c}\mathrm{Ln}(a)\left(\vartheta_2-2\sqrt{\frac{\vartheta_1}{\vartheta_3}}\vartheta_3\mathrm{Cot}_a\left(\sqrt{\vartheta_1\vartheta_3}\eta\right)\right)}{\sqrt{\left(\vartheta_2^2-4\vartheta_1\vartheta_3\right)(-\mathrm{Ln}(a)^2)}})^2+\frac{c}{\delta}\Big]e^{(\kappa\mathbb{B}(t)-\frac{1}{2}\kappa^2 t)}. \tag{4.36}$$

• The combined trigonometric form of solutions

Cluster 13:

$$\Theta_{13}(x,t)=\Big[\frac{\sqrt{2}\,\sqrt{c}\mathrm{Ln}(a)\left(2\sqrt{\frac{\vartheta_1}{\vartheta_3}}\vartheta_3\left(\sqrt{mn}\mathrm{Sec}_a\left(2\sqrt{\vartheta_1\vartheta_3}\eta\right)+\mathrm{Tan}_a\left(2\sqrt{\vartheta_1\vartheta_3}\eta\right)\right)+\vartheta_2\right)}{\sqrt{\left(\vartheta_2^2-4\vartheta_1\vartheta_3\right)(-\mathrm{Ln}(a)^2)}}\Big]e^{(\kappa\mathbb{B}(t)-\frac{1}{2}\kappa^2 t)}. \tag{4.37}$$

$$\phi_{13}(x,t)=\int\Big[\frac{1}{2\delta}(\frac{\sqrt{2}\,\sqrt{c}\mathrm{Ln}(a)\left(2\sqrt{\frac{\vartheta_1}{\vartheta_3}}\vartheta_3\left(\sqrt{mn}\mathrm{Sec}_a\left(2\sqrt{\vartheta_1\vartheta_3}\eta\right)+\mathrm{Tan}_a\left(2\sqrt{\vartheta_1\vartheta_3}\eta\right)\right)+\vartheta_2\right)}{\sqrt{\left(\vartheta_2^2-4\vartheta_1\vartheta_3\right)(-\mathrm{Ln}(a)^2)}})^2+\frac{c}{\delta}\Big]e^{(\kappa\mathbb{B}(t)-\frac{1}{2}\kappa^2 t)}. \tag{4.38}$$

Cluster 14:

$$\Theta_{14}(x,t)=\Big[\frac{\sqrt{2}\,\sqrt{c}\mathrm{Ln}(a)\left(\vartheta_2-2\sqrt{\frac{\vartheta_1}{\vartheta_3}}\vartheta_3\left(\mathrm{Cot}_a\left(2\sqrt{\vartheta_1\vartheta_3}\eta\right)-\sqrt{mn}\mathrm{Csc}_a\left(2\sqrt{\vartheta_1\vartheta_3}\eta\right)\right)\right)}{\sqrt{\left(\vartheta_2^2-4\vartheta_1\vartheta_3\right)(-\mathrm{Ln}(a)^2)}}\Big]e^{(\kappa\mathbb{B}(t)-\frac{1}{2}\kappa^2 t)}. \tag{4.39}$$

$$\phi_{14}(x,t)=\int\Big[\frac{1}{2\delta}(\frac{\sqrt{2}\,\sqrt{c}\mathrm{Ln}(a)\left(\vartheta_2-2\sqrt{\frac{\vartheta_1}{\vartheta_3}}\vartheta_3\left(\mathrm{Cot}_a\left(2\sqrt{\vartheta_1\vartheta_3}\eta\right)-\sqrt{mn}\mathrm{Csc}_a\left(2\sqrt{\vartheta_1\vartheta_3}\eta\right)\right)\right)}{\sqrt{\left(\vartheta_2^2-4\vartheta_1\vartheta_3\right)(-\mathrm{Ln}(a)^2)}})^2+\frac{c}{\delta}\Big]e^{(\kappa\mathbb{B}(t)-\frac{1}{2}\kappa^2 t)}. \tag{4.40}$$

Cluster 15:

$$\Theta_{15}(x,t)=\Big[\frac{\sqrt{2}\,\sqrt{c}\mathrm{Ln}(a)\left(\sqrt{\frac{\vartheta_1}{\vartheta_3}}\vartheta_3\left(\mathrm{Tan}_a\left(\frac{1}{2}\sqrt{\vartheta_1\vartheta_3}\eta\right)-\mathrm{Cot}_a\left(\frac{1}{2}\sqrt{\vartheta_1\vartheta_3}\eta\right)\right)+\vartheta_2\right)}{\sqrt{\left(\vartheta_2^2-4\vartheta_1\vartheta_3\right)(-\mathrm{Ln}(a)^2)}}\Big]e^{(\kappa\mathbb{B}(t)-\frac{1}{2}\kappa^2 t)}. \tag{4.41}$$

$$\phi_{15}(x,t)=\int\Big[\frac{1}{2\delta}(\frac{\sqrt{2}\,\sqrt{c}\mathrm{Ln}(a)\left(\sqrt{\frac{\vartheta_1}{\vartheta_3}}\vartheta_3\left(\mathrm{Tan}_a\left(\frac{1}{2}\sqrt{\vartheta_1\vartheta_3}\eta\right)-\mathrm{Cot}_a\left(\frac{1}{2}\sqrt{\vartheta_1\vartheta_3}\eta\right)\right)+\vartheta_2\right)}{\sqrt{\left(\vartheta_2^2-4\vartheta_1\vartheta_3\right)(-\mathrm{Ln}(a)^2)}})^2+\frac{c}{\delta}\Big]e^{(\kappa\mathbb{B}(t)-\frac{1}{2}\kappa^2 t)}. \tag{4.42}$$

(4) For $\vartheta_1\vartheta_3<0$ and $\vartheta_3=0$.

• The dark soliton solutions

Cluster 16:

$$\Theta_{16}(x,t)=\Big[\frac{\sqrt{2}\,\sqrt{c}\mathrm{Ln}(a)\left(\vartheta_2-2\sqrt{-\frac{\vartheta_1}{\vartheta_3}}\vartheta_3\mathrm{Tanh}_a\left(\sqrt{-\vartheta_1\vartheta_3}\eta\right)\right)}{\sqrt{\left(\vartheta_2^2-4\vartheta_1\vartheta_3\right)(-\mathrm{Ln}(a)^2)}}\Big]e^{(\kappa\mathbb{B}(t)-\frac{1}{2}\kappa^2 t)}. \tag{4.43}$$

$$\phi_{16}(x,t)=\int\Big[\frac{1}{2\delta}(\frac{\sqrt{2}\,\sqrt{c}\mathrm{Ln}(a)\left(\vartheta_2-2\sqrt{-\frac{\vartheta_1}{\vartheta_3}}\vartheta_3\mathrm{Tanh}_a\left(\sqrt{-\vartheta_1\vartheta_3}\eta\right)\right)}{\sqrt{\left(\vartheta_2^2-4\vartheta_1\vartheta_3\right)(-\mathrm{Ln}(a)^2)}})^2+\frac{c}{\delta}\Big]e^{(\kappa\mathbb{B}(t)-\frac{1}{2}\kappa^2 t)}. \tag{4.44}$$

• The singular solitary wave solution

Cluster 17:

$$\Theta_{17}(x,t)=\Big[\frac{\sqrt{2}\,\sqrt{c}\mathrm{Ln}(a)\left(\vartheta_2-2\sqrt{-\frac{\vartheta_1}{\vartheta_3}}\vartheta_3\mathrm{Coth}_a\left(\sqrt{-\vartheta_1\vartheta_3}\eta\right)\right)}{\sqrt{\left(\vartheta_2^2-4\vartheta_1\vartheta_3\right)(-\mathrm{Ln}(a)^2)}}\Big]e^{(\kappa\mathbb{B}(t)-\frac{1}{2}\kappa^2 t)}. \tag{4.45}$$

$$\phi_{17}(x,t)=\int\Big[\frac{1}{2\delta}(\frac{\sqrt{2}\,\sqrt{c}\mathrm{Ln}(a)\left(\vartheta_2-2\sqrt{-\frac{\vartheta_1}{\vartheta_3}}\vartheta_3\mathrm{Coth}_a\left(\sqrt{-\vartheta_1\vartheta_3}\eta\right)\right)}{\sqrt{\left(\vartheta_2^2-4\vartheta_1\vartheta_3\right)(-\mathrm{Ln}(a)^2)}})^2+\frac{c}{\delta}\Big]e^{(\kappa\mathbb{B}(t)-\frac{1}{2}\kappa^2 t)}. \tag{4.46}$$

• Complexiton mixed-type solutions

Cluster 18:

$$\Theta_{18}(x,t)=\Big[\frac{\sqrt{2}\,\sqrt{c}\mathrm{Ln}(a)\left(\vartheta_2+2i\sqrt{-\frac{\vartheta_1}{\vartheta_3}}\vartheta_3\left(\sqrt{mn}\mathrm{Sech}_a\left(2\sqrt{-\vartheta_1\vartheta_3}\eta\right)+i\mathrm{Tanh}_a\left(2\sqrt{-\vartheta_1\vartheta_3}\eta\right)\right)\right)}{\sqrt{\left(\vartheta_2^2-4\vartheta_1\vartheta_3\right)(-\mathrm{Ln}(a)^2)}}\Big]e^{(\kappa\mathbb{B}(t)-\frac{1}{2}\kappa^2 t)} \tag{4.47}$$

$$\phi_{18}(x,t)=\int\Big[\frac{1}{2\delta}(\frac{\sqrt{2}\,\sqrt{c}\mathrm{Ln}(a)\left(\vartheta_2+2i\sqrt{-\frac{\vartheta_1}{\vartheta_3}}\vartheta_3\left(\sqrt{mn}\mathrm{Sech}_a\left(2\sqrt{-\vartheta_1\vartheta_3}\eta\right)+i\mathrm{Tanh}_a\left(2\sqrt{-\vartheta_1\vartheta_3}\eta\right)\right)\right)}{\sqrt{\left(\vartheta_2^2-4\vartheta_1\vartheta_3\right)(-\mathrm{Ln}(a)^2)}})^2+\frac{c}{\delta}\Big]e^{(\kappa\mathbb{B}(t)-\frac{1}{2}\kappa^2 t)} \tag{4.48}$$

Cluster 19:

$$\Theta_{19}(x,t)=\Big[\frac{\sqrt{2}\,\sqrt{c}\mathrm{Ln}(a)\left(\vartheta_2-2\sqrt{-\frac{\vartheta_1}{\vartheta_3}}\vartheta_3\left(\mathrm{Coth}_a\left(2\sqrt{-\vartheta_1\vartheta_3}\eta\right)-\sqrt{mn}\mathrm{Csch}_a\left(2\sqrt{-\vartheta_1\vartheta_3}\eta\right)\right)\right)}{\sqrt{\left(\vartheta_2^2-4\vartheta_1\vartheta_3\right)(-\mathrm{Ln}(a)^2)}}\Big]e^{(\kappa\mathbb{B}(t)-\frac{1}{2}\kappa^2 t)}. \tag{4.49}$$

$$\phi_{19}(x,t)=\int\Big[\frac{1}{2\delta}(\frac{\sqrt{2}\,\sqrt{c}\mathrm{Ln}(a)\left(\vartheta_2-2\sqrt{-\frac{\vartheta_1}{\vartheta_3}}\vartheta_3\left(\mathrm{Coth}_a\left(2\sqrt{-\vartheta_1\vartheta_3}\eta\right)-\sqrt{mn}\mathrm{Csch}_a\left(2\sqrt{-\vartheta_1\vartheta_3}\eta\right)\right)\right)}{\sqrt{\left(\vartheta_2^2-4\vartheta_1\vartheta_3\right)(-\mathrm{Ln}(a)^2)}})^2+\frac{c}{\delta}\Big]e^{(\kappa\mathbb{B}(t)-\frac{1}{2}\kappa^2 t)}. \tag{4.50}$$

Cluster 20:

$$\Theta_{20}(x,t)=\Big[\frac{\sqrt{2}\,\sqrt{c}\mathrm{Ln}(a)\left(\frac{\vartheta_1\left(\mathrm{Coth}_a\left(\sqrt{-\vartheta_1\vartheta_3}\eta\right)+\mathrm{Tanh}_a\left(\sqrt{-\vartheta_1\vartheta_3}\eta\right)\right)}{\sqrt{-\frac{\vartheta_1}{\vartheta_3}}}+\vartheta_2\right)}{\sqrt{\left(\vartheta_2^2-4\vartheta_1\vartheta_3\right)(-\mathrm{Ln}(a)^2)}}\Big]e^{(\kappa\mathbb{B}(t)-\frac{1}{2}\kappa^2 t)}. \tag{4.51}$$

$$\phi_{20}(x,t)=\int\Big[\frac{1}{2\delta}(\frac{\sqrt{2}\,\sqrt{c}\mathrm{Ln}(a)\left(\frac{\vartheta_1\left(\mathrm{Coth}_a\left(\sqrt{-\vartheta_1\vartheta_3}\eta\right)+\mathrm{Tanh}_a\left(\sqrt{-\vartheta_1\vartheta_3}\eta\right)\right)}{\sqrt{-\frac{\vartheta_1}{\vartheta_3}}}+\vartheta_2\right)}{\sqrt{\left(\vartheta_2^2-4\vartheta_1\vartheta_3\right)(-\mathrm{Ln}(a)^2)}})^2+\frac{c}{\delta}\Big]e^{(\kappa\mathbb{B}(t)-\frac{1}{2}\kappa^2 t)}. \tag{4.52}$$

(5) For $\vartheta_2=0$ and $\vartheta_1=\vartheta_3$.

• The solutions for periodic waves

Cluster 21:

$$\Theta_{21}(x,t)=\Big[\frac{\sqrt{2}\,\sqrt{c}\mathrm{Ln}(a)\left(2\vartheta_3\mathrm{Tan}_a\left(\vartheta_1\eta\right)+\vartheta_2\right)}{\sqrt{\left(\vartheta_2^2-4\vartheta_1\vartheta_3\right)(-\mathrm{Ln}(a)^2)}}\Big]e^{(\kappa\mathbb{B}(t)-\frac{1}{2}\kappa^2 t)}. \tag{4.53}$$

$$\phi_{21}(x,t)=\int\left[\frac{1}{2\delta}(\frac{\sqrt{2}\,\sqrt{c}\mathrm{Ln}(a)\,(2\vartheta_3\mathrm{Tan}_a\,(\vartheta_1\eta)+\vartheta_2)}{\sqrt{\left(\vartheta_2^2-4\vartheta_1\vartheta_3\right)(-\mathrm{Ln}(a)^2)}})^2+\frac{c}{\delta}\right]e^{(\kappa\mathbb{B}(t)-\frac{1}{2}\kappa^2 t)}. \tag{4.54}$$

Cluster 22:

$$\Theta_{22}(x,t)=\left[\frac{\sqrt{2}\,\sqrt{c}\mathrm{Ln}(a)\,(\vartheta_2-2\vartheta_3\mathrm{Cot}_a\,(\vartheta_1\eta))}{\sqrt{\left(\vartheta_2^2-4\vartheta_1\vartheta_3\right)(-\mathrm{Ln}(a)^2)}}\right]e^{(\kappa\mathbb{B}(t)-\frac{1}{2}\kappa^2 t)}. \tag{4.55}$$

$$\phi_{22}(x,t)=\int\left[\frac{1}{2\delta}(\frac{\sqrt{2}\,\sqrt{c}\mathrm{Ln}(a)\,(\vartheta_2-2\vartheta_3\mathrm{Cot}_a\,(\vartheta_1\eta))}{\sqrt{\left(\vartheta_2^2-4\vartheta_1\vartheta_3\right)(-\mathrm{Ln}(a)^2)}})^2+\frac{c}{\delta}\right]e^{(\kappa\mathbb{B}(t)-\frac{1}{2}\kappa^2 t)}. \tag{4.56}$$

• Combined trigonometric solutions

Cluster 23:

$$\Theta_{23}(x,t)=\left[\frac{\sqrt{2}\,\sqrt{c}\mathrm{Ln}(a)\left(2\vartheta_3\left(\sqrt{mn}\mathrm{Sec}_a\,(2\vartheta_1\eta)+\mathrm{Tan}_a\,(2\vartheta_1\eta)\right)+\vartheta_2\right)}{\sqrt{\left(\vartheta_2^2-4\vartheta_1\vartheta_3\right)(-\mathrm{Ln}(a)^2)}}\right]e^{(\kappa\mathbb{B}(t)-\frac{1}{2}\kappa^2 t)}. \tag{4.57}$$

$$\phi_{23}(x,t)=\int\left[\frac{1}{2\delta}(\frac{\sqrt{2}\,\sqrt{c}\mathrm{Ln}(a)\left(2\vartheta_3\left(\sqrt{mn}\mathrm{Sec}_a\,(2\vartheta_1\eta)+\mathrm{Tan}_a\,(2\vartheta_1\eta)\right)+\vartheta_2\right)}{\sqrt{\left(\vartheta_2^2-4\vartheta_1\vartheta_3\right)(-\mathrm{Ln}(a)^2)}})^2+\frac{c}{\delta}\right]e^{(\kappa\mathbb{B}(t)-\frac{1}{2}\kappa^2 t)}. \tag{4.58}$$

Cluster 24:

$$\Theta_{24}(x,t)=\left[\frac{\sqrt{2}\,\sqrt{c}\mathrm{Ln}(a)\left(\vartheta_2-2\vartheta_3\left(\mathrm{Cot}_a\,(2\vartheta_1\eta)-\sqrt{mn}\mathrm{Csc}_a\,(2\vartheta_1\eta)\right)\right)}{\sqrt{\left(\vartheta_2^2-4\vartheta_1\vartheta_3\right)(-\mathrm{Ln}(a)^2)}}\right]e^{(\kappa\mathbb{B}(t)-\frac{1}{2}\kappa^2 t)}. \tag{4.59}$$

$$\phi_{24}(x,t)=\int\left[\frac{1}{2\delta}(\frac{\sqrt{2}\,\sqrt{c}\mathrm{Ln}(a)\left(\vartheta_2-2\vartheta_3\left(\mathrm{Cot}_a\,(2\vartheta_1\eta)-\sqrt{mn}\mathrm{Csc}_a\,(2\vartheta_1\eta)\right)\right)}{\sqrt{\left(\vartheta_2^2-4\vartheta_1\vartheta_3\right)(-\mathrm{Ln}(a)^2)}})^2+\frac{c}{\delta}\right]e^{(\kappa\mathbb{B}(t)-\frac{1}{2}\kappa^2 t)}. \tag{4.60}$$

Cluster 25:

$$\Theta_{25}(x,t)=\left[\frac{\sqrt{2}\,\sqrt{c}\mathrm{Ln}(a)\left(\vartheta_3\left(\mathrm{Tan}_a\left(\frac{\vartheta_1\eta}{2}\right)-\mathrm{Cot}_a\left(\frac{\vartheta_1\eta}{2}\right)\right)+\vartheta_2\right)}{\sqrt{\left(\vartheta_2^2-4\vartheta_1\vartheta_3\right)(-\mathrm{Ln}(a)^2)}}\right]e^{(\kappa\mathbb{B}(t)-\frac{1}{2}\kappa^2 t)}. \tag{4.61}$$

$$\phi_{25}(x,t)=\int\left[\frac{1}{2\delta}(\frac{\sqrt{2}\,\sqrt{c}\mathrm{Ln}(a)\left(\vartheta_3\left(\mathrm{Tan}_a\left(\frac{\vartheta_1\eta}{2}\right)-\mathrm{Cot}_a\left(\frac{\vartheta_1\eta}{2}\right)\right)+\vartheta_2\right)}{\sqrt{\left(\vartheta_2^2-4\vartheta_1\vartheta_3\right)(-\mathrm{Ln}(a)^2)}})^2+\frac{c}{\delta}\right]e^{(\kappa\mathbb{B}(t)-\frac{1}{2}\kappa^2 t)}. \tag{4.62}$$

(6) For $\vartheta_2=0$ and $\vartheta_1=-\vartheta_3$.

• Exact wave solutions

Cluster 26:

$$\Theta_{26}(x,t)=\left[\frac{\sqrt{2}\,\sqrt{c}\mathrm{Ln}(a)\,(\vartheta_2-2\vartheta_3\mathrm{Tanh}_a\,(\vartheta_1\eta))}{\sqrt{\left(\vartheta_2^2-4\vartheta_1\vartheta_3\right)(-\mathrm{Ln}(a)^2)}}\right]e^{(\kappa\mathbb{B}(t)-\frac{1}{2}\kappa^2 t)}. \tag{4.63}$$

$$\phi_{26}(x,t)=\int\left[\frac{1}{2\delta}(\frac{\sqrt{2}\,\sqrt{c}\mathrm{Ln}(a)\left(\vartheta_2-2\vartheta_3\mathrm{Tanh}_a\left(\vartheta_1\eta\right)\right)}{\sqrt{\left(\vartheta_2^2-4\vartheta_1\vartheta_3\right)\left(-\mathrm{Ln}(a)^2\right)}})^2+\frac{c}{\delta}\right]e^{(\kappa\mathbb{B}(t)-\frac{1}{2}\kappa^2t)}. \tag{4.64}$$

Cluster 27:

$$\Theta_{27}(x,t)=\left[\frac{\sqrt{2}\,\sqrt{c}\mathrm{Ln}(a)\left(\vartheta_2-2\vartheta_3\mathrm{Coth}_a\left(\vartheta_1\eta\right)\right)}{\sqrt{\left(\vartheta_2^2-4\vartheta_1\vartheta_3\right)\left(-\mathrm{Ln}(a)^2\right)}}\right]e^{(\kappa\mathbb{B}(t)-\frac{1}{2}\kappa^2t)}. \tag{4.65}$$

$$\phi_{27}(x,t)=\int\left[\frac{1}{2\delta}(\frac{\sqrt{2}\,\sqrt{c}\mathrm{Ln}(a)\left(\vartheta_2-2\vartheta_3\mathrm{Coth}_a\left(\vartheta_1\eta\right)\right)}{\sqrt{\left(\vartheta_2^2-4\vartheta_1\vartheta_3\right)\left(-\mathrm{Ln}(a)^2\right)}})^2+\frac{c}{\delta}\right]e^{(\kappa\mathbb{B}(t)-\frac{1}{2}\kappa^2t)}. \tag{4.66}$$

Cluster 28:

$$\Theta_{28}(x,t)=\left[\frac{\sqrt{2}\,\sqrt{c}\mathrm{Ln}(a)\left(\vartheta_2+2i\vartheta_3\left(\sqrt{mn}\mathrm{Sech}_a\left(2\vartheta_1\eta\right)+i\mathrm{Tanh}_a\left(2\vartheta_1\eta\right)\right)\right)}{\sqrt{\left(\vartheta_2^2-4\vartheta_1\vartheta_3\right)\left(-\mathrm{Ln}(a)^2\right)}}\right]e^{(\kappa\mathbb{B}(t)-\frac{1}{2}\kappa^2t)}. \tag{4.67}$$

$$\phi_{28}(x,t)=\int\left[\frac{1}{2\delta}(\frac{\sqrt{2}\,\sqrt{c}\mathrm{Ln}(a)\left(\vartheta_2+2i\vartheta_3\left(\sqrt{mn}\mathrm{Sech}_a\left(2\vartheta_1\eta\right)+i\mathrm{Tanh}_a\left(2\vartheta_1\eta\right)\right)\right)}{\sqrt{\left(\vartheta_2^2-4\vartheta_1\vartheta_3\right)\left(-\mathrm{Ln}(a)^2\right)}})^2+\frac{c}{\delta}\right]e^{(\kappa\mathbb{B}(t)-\frac{1}{2}\kappa^2t)}. \tag{4.68}$$

Cluster 29:

$$\Theta_{29}(x,t)=\left[\frac{\sqrt{2}\,\sqrt{c}\mathrm{Ln}(a)\left(\vartheta_2-\vartheta_3\left(\mathrm{Coth}_a\left(2\vartheta_1\eta\right)+\mathrm{Csch}_a\left(2\vartheta_1\eta\right)\right)\right)}{\sqrt{\left(\vartheta_2^2-4\vartheta_1\vartheta_3\right)\left(-\mathrm{Ln}(a)^2\right)}}\right]e^{(\kappa\mathbb{B}(t)-\frac{1}{2}\kappa^2t)}. \tag{4.69}$$

$$\phi_{29}(x,t)=\int\left[\frac{1}{2\delta}(\frac{\sqrt{2}\,\sqrt{c}\mathrm{Ln}(a)\left(\vartheta_2-\vartheta_3\left(\mathrm{Coth}_a\left(2\vartheta_1\eta\right)+\mathrm{Csch}_a\left(2\vartheta_1\eta\right)\right)\right)}{\sqrt{\left(\vartheta_2^2-4\vartheta_1\vartheta_3\right)\left(-\mathrm{Ln}(a)^2\right)}})^2+\frac{c}{\delta}\right]e^{(\kappa\mathbb{B}(t)-\frac{1}{2}\kappa^2t)}. \tag{4.70}$$

Cluster 30:

$$\Theta_{30}(x,t)=\left[\frac{\sqrt{2}\,\sqrt{c}\mathrm{Ln}(a)\left(\vartheta_2-\vartheta_3\left(\mathrm{Coth}_a\left(\frac{\vartheta_1\eta}{2}\right)+\mathrm{Tanh}_a\left(\frac{\vartheta_1\eta}{2}\right)\right)\right)}{\sqrt{\left(\vartheta_2^2-4\vartheta_1\vartheta_3\right)\left(-\mathrm{Ln}(a)^2\right)}}\right]e^{(\kappa\mathbb{B}(t)-\frac{1}{2}\kappa^2t)}. \tag{4.71}$$

$$\phi_{30}(x,t)=\int\left[\frac{\sqrt{2}\,\sqrt{c}\mathrm{Ln}(a)\left(\vartheta_2-\vartheta_3\left(\mathrm{Coth}_a\left(\frac{\vartheta_1\eta}{2}\right)+\mathrm{Tanh}_a\left(\frac{\vartheta_1\eta}{2}\right)\right)\right)}{\sqrt{\left(\vartheta_2^2-4\vartheta_1\vartheta_3\right)\left(-\mathrm{Ln}(a)^2\right)}}\frac{1}{2\delta}()^2+\frac{c}{\delta}\right]e^{(\kappa\mathbb{B}(t)-\frac{1}{2}\kappa^2t)}. \tag{4.72}$$

(7) For $\vartheta_2^2=4\vartheta_1\vartheta_3$.

• Rational function solution

Cluster 31:

$$\Theta_{31}(x,t)=\left[\frac{\sqrt{2}\,\sqrt{c}\left(\vartheta_2^2\eta\mathrm{Ln}(a)-2\vartheta_1\left(\vartheta_2\eta\mathrm{Ln}(a)+2\right)\right)}{\vartheta_2\eta\sqrt{\left(\vartheta_2^2-4\vartheta_1\vartheta_3\right)\left(-\mathrm{Ln}(a)^2\right)}}\right]e^{(\kappa\mathbb{B}(t)-\frac{1}{2}\kappa^2t)}. \tag{4.73}$$

$$\phi_{31}(x,t)=\int\left[\frac{1}{2\delta}(\frac{\sqrt{2}\,\sqrt{c}\left(\vartheta_2^2\eta\mathrm{Ln}(a)-2\vartheta_1\left(\vartheta_2\eta\mathrm{Ln}(a)+2\right)\right)}{\vartheta_2\eta\sqrt{\left(\vartheta_2^2-4\vartheta_1\vartheta_3\right)\left(-\mathrm{Ln}(a)^2\right)}})^2+\frac{c}{\delta}\right]e^{(\kappa\mathbb{B}(t)-\frac{1}{2}\kappa^2t)}. \tag{4.74}$$

For all the solutions above, $\eta=\frac{\sqrt{2}\,\sqrt{c}t}{\sqrt{(\vartheta_2^2-4\vartheta_1\vartheta_3)(-\mathrm{Ln}(a)^2)}}+\frac{\alpha x^\beta}{\beta}$.

4.2. Implementation of the improved $\mathscr{F}$-expansion method

According to Eq (5.1),

$$\varsigma(\eta) = \lambda_0 + \lambda_1(\mathscr{F}(\eta) + \mathscr{M}) + \frac{\mu_1}{\mathscr{F}(\eta) + \mathscr{M}}, \tag{4.75}$$

by merging Eqs (4.75) and (3.7) in Eq (4.8), we obtain the following solution sets.
Family I:

$$\lambda_0 \to \lambda_0,\ \lambda_1 \to 0,\ \mu_1 \to -\frac{\lambda_0\left(\mathscr{M}^2 + \mathscr{Q}\right)}{\mathscr{M}},\ c \to \frac{\lambda_0^2\mathscr{Q}}{2\mathscr{M}^2},\ \delta \to \frac{\lambda_0}{2\mathscr{M}}.$$

Family II:

$$\lambda_0 \to \lambda_0,\ \lambda_1 \to -\frac{\lambda_0}{m},\ \mu_1 \to 0,\ c \to \frac{\lambda_0^2 q}{2m^2},\ \delta \to -\frac{\lambda_0}{2m}.$$

For Family I
• If $\mathscr{Q} < 0$, then

$$\Theta_1(x,t) = \left[\lambda_0\left(1 - \frac{\mathscr{M}^2 + \mathscr{Q}}{\mathscr{M}^2 - \mathscr{M}\sqrt{-\mathscr{Q}}\tanh\left(\sqrt{-\mathscr{Q}}\left(\frac{\lambda_0 t}{2\mathscr{M}} + \frac{\alpha x^\beta}{\beta}\right)\right)}\right)\right]e^{(\kappa\mathbb{B}(t) - \frac{1}{2}\kappa^2 t)}, \tag{4.76}$$

$$\phi_1(x,t) = \int\left[\frac{1}{2\delta}(\lambda_0\left(1 - \frac{\mathscr{M}^2 + \mathscr{Q}}{\mathscr{M}^2 - \mathscr{M}\sqrt{-\mathscr{Q}}\tanh\left(\sqrt{-\mathscr{Q}}\left(\frac{\lambda_0 t}{2\mathscr{M}} + \frac{\alpha x^\beta}{\beta}\right)\right)}\right))^2 + \frac{c}{\delta}\right]e^{(\kappa\mathbb{B}(t) - \frac{1}{2}\kappa^2 t)}, \tag{4.77}$$

$$\Theta_2(x,t) = \left[\lambda_0\left(1 - \frac{\mathscr{M}^2 + \mathscr{Q}}{\mathscr{M}^2 - \mathscr{M}\sqrt{-\mathscr{Q}}\coth\left(\sqrt{-\mathscr{Q}}\left(\frac{\lambda_0 t}{2\mathscr{M}} + \frac{\alpha x^\beta}{\beta}\right)\right)}\right)\right]e^{(\kappa\mathbb{B}(t) - \frac{1}{2}\kappa^2 t)}, \tag{4.78}$$

$$\phi_2(x,t) = \int\left[\frac{1}{2\delta}(\lambda_0\left(1 - \frac{\mathscr{M}^2 + \mathscr{Q}}{\mathscr{M}^2 - \mathscr{M}\sqrt{-\mathscr{Q}}\coth\left(\sqrt{-\mathscr{Q}}\left(\frac{\lambda_0 t}{2\mathscr{M}} + \frac{\alpha x^\beta}{\beta}\right)\right)}\right))^2 + \frac{c}{\delta}\right]e^{(\kappa\mathbb{B}(t) - \frac{1}{2}\kappa^2 t)}. \tag{4.79}$$

• If $\mathscr{Q} > 0$, then

$$\Theta_3(x,t) = \left[\lambda_0\left(1 - \frac{\mathscr{M}^2 + \mathscr{Q}}{\mathscr{M}^2 + \mathscr{M}\sqrt{\mathscr{Q}}\tan\left(\sqrt{\mathscr{Q}}\left(\frac{\lambda_0 t}{2\mathscr{M}} + \frac{\alpha x^\beta}{\beta}\right)\right)}\right)\right]e^{(\kappa\mathbb{B}(t) - \frac{1}{2}\kappa^2 t)}, \tag{4.80}$$

$$\phi_3(x,t) = \int\left[\frac{1}{2\delta}(\lambda_0\left(1 - \frac{\mathscr{M}^2 + \mathscr{Q}}{\mathscr{M}^2 + \mathscr{M}\sqrt{\mathscr{Q}}\tan\left(\sqrt{\mathscr{Q}}\left(\frac{\lambda_0 t}{2\mathscr{M}} + \frac{\alpha x^\beta}{\beta}\right)\right)}\right))^2 + \frac{c}{\delta}\right]e^{(\kappa\mathbb{B}(t) - \frac{1}{2}\kappa^2 t)}, \tag{4.81}$$

$$\Theta_4(x,t) = \left[\lambda_0\left(1 - \frac{\mathscr{M}^2 + q}{\mathscr{M}^2 - \mathscr{M}\sqrt{\mathscr{Q}}\cot\left(\sqrt{\mathscr{Q}}\left(\frac{\lambda_0 t}{2\mathscr{M}} + \frac{\alpha x^\beta}{\beta}\right)\right)}\right)\right]e^{(\kappa\mathbb{B}(t) - \frac{1}{2}\kappa^2 t)}, \tag{4.82}$$

$$\phi_4(x,t) = \int \left[\frac{1}{2\delta}(\lambda_0\left(1 - \frac{\mathscr{M}^2 + q}{\mathscr{M}^2 - \mathscr{M}\sqrt{\mathscr{Q}}\cot\left(\sqrt{\mathscr{Q}}\left(\frac{\lambda_0 t}{2\mathscr{M}} + \frac{\alpha x^\beta}{\beta}\right)\right)}\right)^2 + \frac{c}{\delta}\right] e^{(\kappa\mathbb{B}(t) - \frac{1}{2}\kappa^2 t)}. \tag{4.83}$$

• If $\mathscr{Q} = 0$, then

$$\Theta_5(x,t) = \left[\lambda_0\left(1 - \frac{\mathscr{M}^2 + \mathscr{Q}}{\mathscr{M}\left(\mathscr{M} - \frac{2\beta\mathscr{M}}{2\alpha\mathscr{M}x^\beta + \beta\lambda_0 t}\right)}\right)\right] e^{(\kappa\mathbb{B}(t) - \frac{1}{2}\kappa^2 t)}, \tag{4.84}$$

$$\phi_5(x,t) = \int \left[\frac{1}{2\delta}(\lambda_0\left(1 - \frac{\mathscr{M}^2 + \mathscr{Q}}{\mathscr{M}\left(\mathscr{M} - \frac{2\beta\mathscr{M}}{2\alpha\mathscr{M}x^\beta + \beta\lambda_0 t}\right)}\right)^2 + \frac{c}{\delta}\right] e^{(\kappa\mathbb{B}(t) - \frac{1}{2}\kappa^2 t)}. \tag{4.85}$$

5. Sensitivity analysis

This section conducts and in-depth sensitivity analysis in depth for the dynamic system defined by Eq (4.8) [34]. We must first resolve the system shown below:

$$\begin{cases} \frac{d\varsigma}{d\eta} = \mathscr{R}(\eta) = \mathfrak{L}_1, \\ \frac{d\mathscr{R}}{d\eta} = \mathscr{A}\mathscr{R}^3(\eta) + \mathscr{B}\mathscr{R}(\eta) = \mathfrak{L}_2, \end{cases} \tag{5.1}$$

where $\mathscr{A} = \frac{1}{2\delta^2}$ and $\mathscr{B} = \frac{c}{2\delta^2}$. We use various parameter values ($c = -0.2$ *and* $\delta = 0.4$) to observe how much the system exhibits variations in its dynamics. Figure 1 represents two solutions: $(\mathfrak{L}_1, \mathfrak{L}_2) = (0.03, 0)$ on the gray line, $(\mathfrak{L}_1, \mathfrak{L}_2) = (0, 0.09)$ on the yellow line. Figure 2 represents two solutions: $(\mathfrak{L}_1, \mathfrak{L}_2) = (0, 0)$ on the blue line, $(\mathfrak{L}_1, \mathfrak{L}_2) = (0, -0.02)$ on the yellow line. Similarly, Figure 3 represents three solutions: $(\mathfrak{L}_1, \mathfrak{L}_2) = (-0.04, -0.04)$ on the black line, $(\mathfrak{L}_1, \mathfrak{L}_2) = (-0.02, -0.02)$ on the yellow line, $(\mathfrak{L}_1, \mathfrak{L}_2) = (-0.03, -0.03)$ on the green line. Sensitivity analysis is essential to the study of dynamic systems. It improves comprehension, guarantees stability, and directs wise decision-making. Whether used to address engineering systems, disease transmission, or climate change, this technology connects theoretical understanding with real-world results. Many disciplines, including science, engineering, and economics, employ sensitivity analysis as a technique to assess how changing the input parameters affects the output of a model. It comprises tracking how the output changes while the input values are gradually changed within a predefined range. Sensitivity analysis finds the input components that have the most impact on the outcomes, which aids in risk assessment, decision-making, and improvement. It is crucial for comprehending and controlling uncertainty in complex systems.

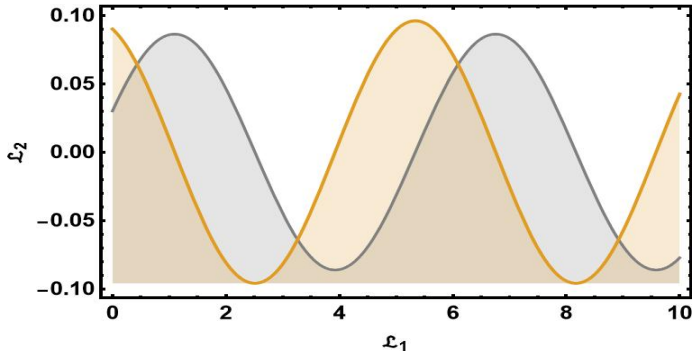

(a)

Figure 1. Sensitivity analysis of the proposed system (5.1) with the initial conditions $(\mathfrak{Q}_1, \mathfrak{Q}_2) = (0.03, 0)$ on the gray line and $(\mathfrak{Q}_1, \mathfrak{Q}_2) = (0, 0.09)$ on the yellow line.

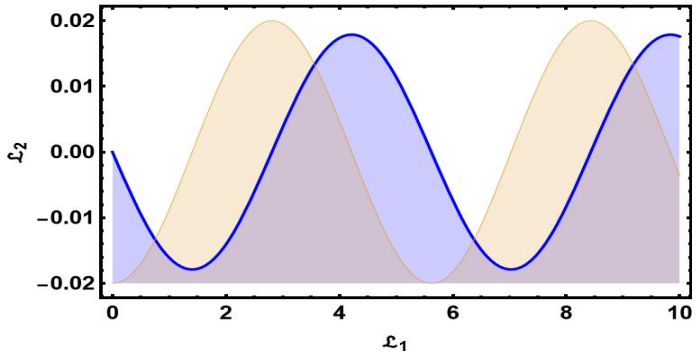

(a)

Figure 2. Sensitivity analysis of the proposed system (5.1) with the initial conditions $(\mathfrak{Q}_1, \mathfrak{Q}_2) = (00)$ on the blue line and $(\mathfrak{Q}_1, \mathfrak{Q}_2) = (0, -0.02)$ on the yellow line.

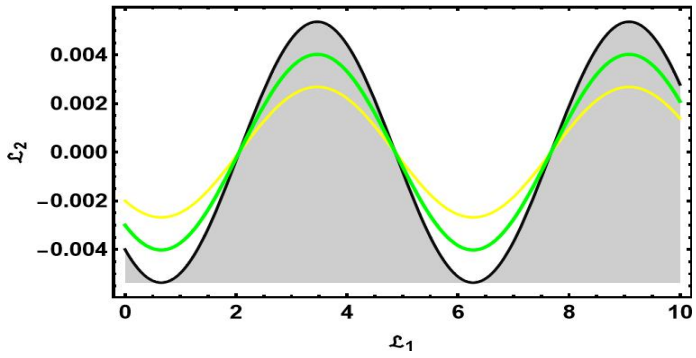

(a)

Figure 3. Sensitivity analysis of the proposed system (5.1) with the initial conditions $(\mathfrak{Q}_1, \mathfrak{Q}_2) = (-0.04, -0.04)$ on the black line, $(\mathfrak{Q}_1, \mathfrak{Q}_2) = (-0.02, -0.02)$ on the yellow line, and $(\mathfrak{Q}_1, \mathfrak{Q}_2) = (-0.03, -0.03)$ on the green line.

6. Results and discussion

This part demonstrates the uniqueness and novelty of the current study by providing a comprehensive comparison of the evaluated results with the calculated outcomes that have already been achieved. In previous work, Wael et al. [25] examined the aforementioned model and found travelling wave solutions using the mapping method. Furthermore, our work's novelty is justified because, upon comparing our results with those previously obtained through various approaches, it becomes evident [28–31] that while some solution types have already been documented in the literature, the majority are new. The current study systematically derived several novel stochastic solitary wave solutions for the fractional stochastic KMMS, employing the NEDAM and the improved $\mathscr{F}$-expansion technique. The analytic forms of dark, dark–bright, bright–dark, periodic, singular, mixed trigonometric, hyperbolic, and rational provide new information about the properties of nonlinear dispersive waves when stochastic factors are present. We also conducted a sensitivity analysis of the selected model by considering the different initial conditions. We provide deeper understanding of the nonlinear dynamics and wave properties of the fractional stochastic KMMS through our range of solutions and graphical representations. In addition to providing useful technological applications, it expands our knowledge of nonlinear dynamics in ferromagnetic materials and strengthens the theoretical underpinnings of fractional calculus and stochastic processes. Our graphical explanations and range of solutions offer additional insights into the nonlinear dynamics and wave features inherent in the subject under investigation. Specifically, Figure 4 shows a distinct graphical structure for the periodic solution of Eq (4.13), reflecting the steady oscillatory behavior frequently found in mechanical systems or optical fibers. Similar to this, Figure 5 visualizes the singular periodic solution of Eq (4.17), indicating the existence of localized energy bursts that might be physical events such as powerful laser pulses in nonlinear optics or rogue waves in oceanography. The dark solution for Eq (4.23) in Figure 6 indicates energy dips in the system, which are a feature frequently seen in dark solitons in optical communication systems or Bose–Einstein condensates. The soliton envelope of Eq (4.27) exhibits secondary peaks in the periodic M-shape solution depicted in Figure 7, which may be indicative of multi-pulse wave interactions in nonlinear media. Figure 8 show trigonometric solutions to Eq (4.53), which are representative of oscillatory processes like alternating currents in electrical systems or pendulum motion. The hyperbolic stochastic solution of Eq (4.65), which is seen in Figure 9, emphasizes the impact of random disturbances in systems like turbulent flows or climate models. The dark stochastic solution of Eq (4.76) is shown in Figure 10, indicating situations in which randomness results in energy reduction or damping effects, which can be crucial in comprehending how noise affects wave propagation. Finally, Eq (4.80) has a periodic stochastic solution, represented in Figure 11, which implies periodic responses in the presence of stochasticity. This solution can be used to simulate physical systems such as population dynamics under environmental fluctuations or randomly driven oscillators. With this explanation, scientists and researchers can better understand the significance of mathematical discoveries. These solutions are important because they allow for the representation of many different types of nonlinear mathematical and physical systems and phenomena, including laser physics and fluid dynamics.

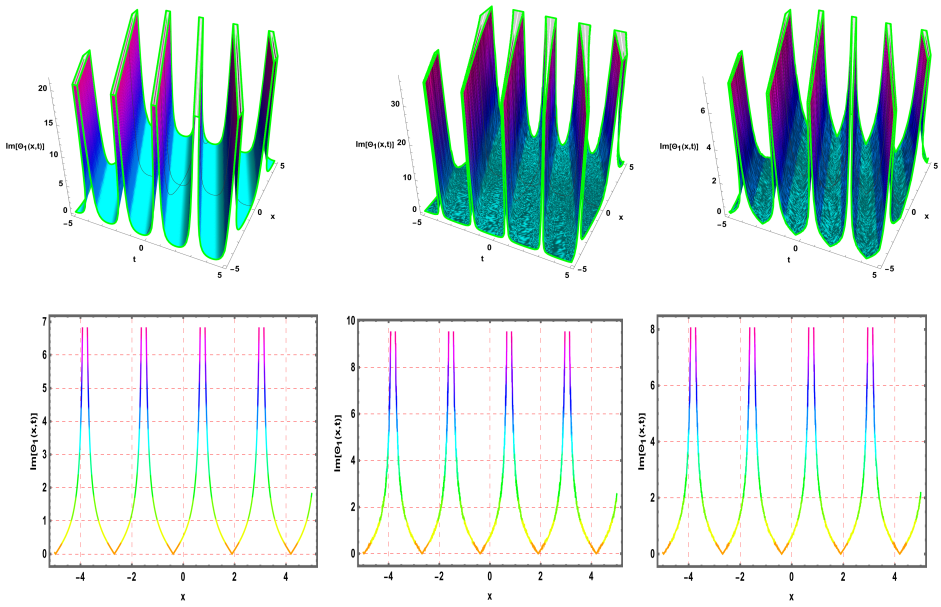

(d) $\beta = 1,\ \omega = 0$ (e) $\beta = 1,\ \omega = 0.7$ (f) $\beta = 1,\ \omega = 0.47$

Figure 4. Dynamic perspective of the solution of (4.13) with the parameters $\vartheta_1 = 3.7,\ \vartheta_2 = -3.1,\ \vartheta_3 = 3.4,\ \alpha = 0.43,\ a = 2.3,\ B(t) = 0.2$, and $c = 0.4$.

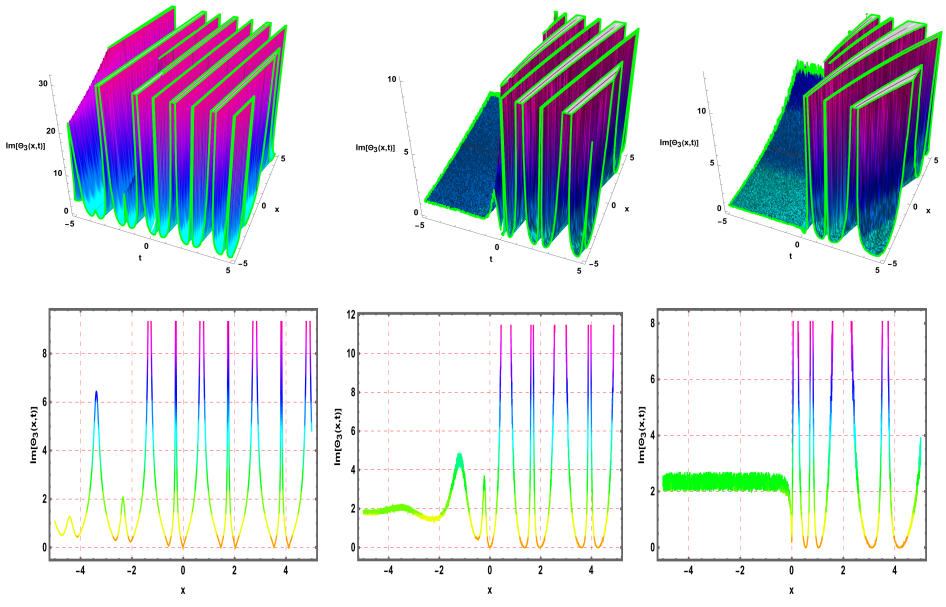

(d) $\beta = 0.99,\ \omega = 0$ (e) $\beta = 0.8,\ \omega = 0.3$ (f) $\beta = 0.5,\ \omega = 0.5$

Figure 5. Dynamic perspective of the solution of (4.17) with the parameters $\vartheta_1 = 3.9,\ \vartheta_2 = -3.52,\ \vartheta_3 = 3.76,\ B(t) = 0.1,\ a = 0.15,\ m = 0.6,\ n = 0.7,\ c = 0.78$, and $\alpha = 0.45$.

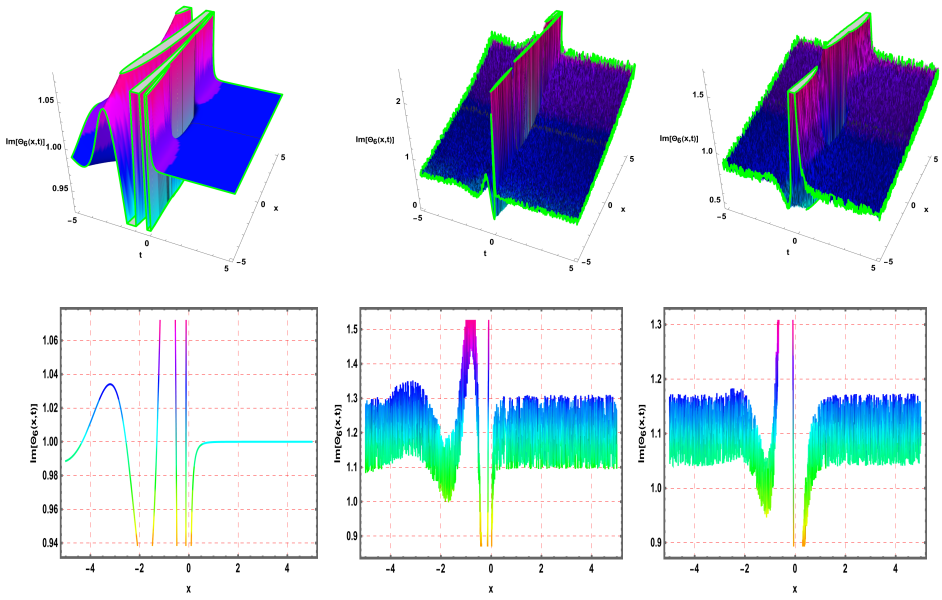

(d) $\beta = 0.4,\ \omega = 0$ (e) $\beta = 0.4,\ \omega = 0.3$ (f) $\beta = 0.7,\ \omega = 0.2$

Figure 6. Dynamic perspective of the solution of (4.23) with the parameters $\vartheta_1 = 3.4,\ \vartheta_2 = 3.6,\ \vartheta_3 = -3.4,,\ c = 0.5,\ \alpha = 0.5; a = 0.3$, and $B(t) = 0.67$.

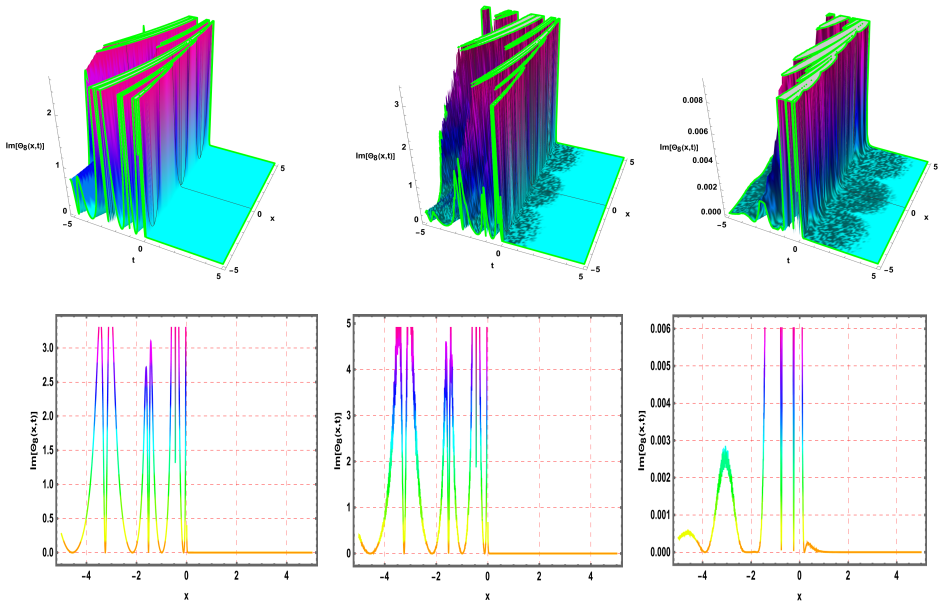

(d) $\beta = 0.49,\ \omega = 0$ (e) $\beta = 0.49,\ \omega = 0.5$ (f) $\beta = 0.59,\ \omega = 0.4$

Figure 7. Dynamic perspective of the solution of (4.27) with the parameters $\vartheta_1 = 5.2,\ \vartheta_2 = 3.4,\ \vartheta_3 = -3.6,\ \alpha = 0.3,\ c = 0.54,\ a = 0.3,\ m = 0.2,\ n = 0.3$, and $B(t) = 0.9$.

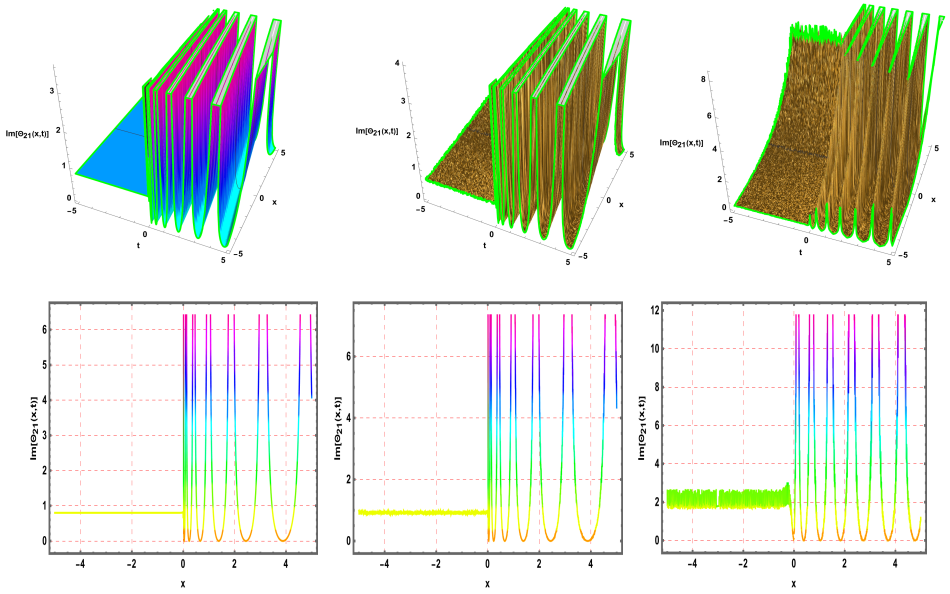

(d) $\beta = 0.4,\ \omega = 0$ (e) $\beta = 0.4,\ \omega = 0.25$ (f) $\beta = 0.74,\ \omega = 0.84$

Figure 8. Dynamic perspective of the solution of (4.53) with the parameters $\vartheta_1 = 5.4,\ \vartheta_2 = 0,\ \vartheta_3 = 5.4,\ c = 0.4,\ \alpha = -0.8,\ B(t) = 0.8$, and $a = 0.2$.

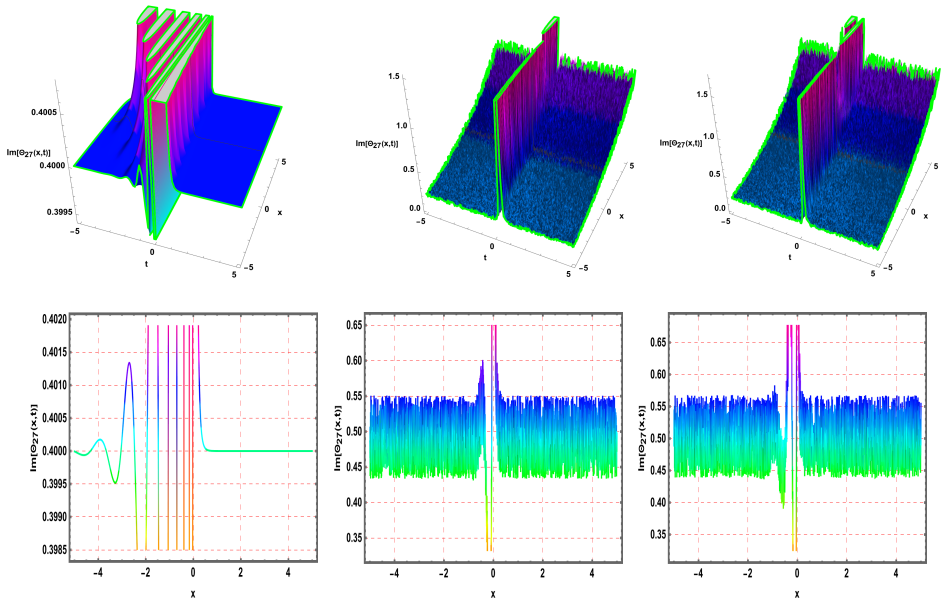

(d) $\beta = 0,\ \omega = 0.6$ (e) $\beta = 0.7,\ \omega = 0.4$ (f) $\beta = 0.63,\ \omega = 0.43$

Figure 9. Dynamic perspective of the solution of (4.65) with the parameters $\vartheta_1 = 2.1,\ \vartheta_2 = 0,\ \vartheta_3 = -5.1,\ c = 0.6,\ \alpha = 0.54,\ B(t) = 3$, and $a = 0.2$.

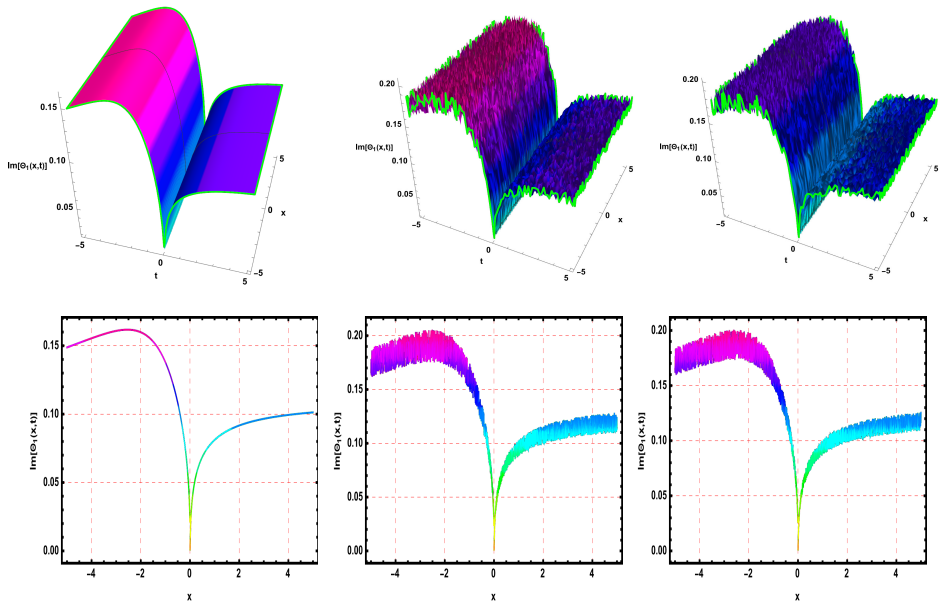

(d) $\beta = 0.3,\ \omega = 0$ (e) $\beta = 0.3,\ \omega = 0.4$ (f) $\beta = 0.3,\ \omega = 0.37$

Figure 10. Dynamic perspective of the solution of (4.76) with the parameters $\alpha = 0.43,\ \lambda_0 = 0.4,\ \mathscr{Q} = -0.7,\ \mathscr{M} = 3.1$, and $B(t) = 3.4$.

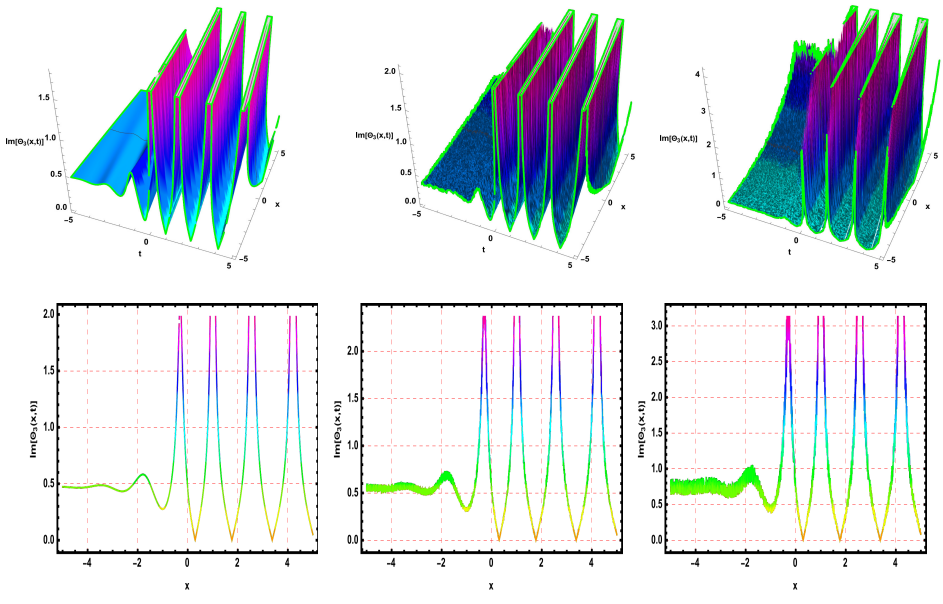

(d) $\beta = 0.91,\ \omega = 0$ (e) $\beta = 0.91,\ \omega = 0.4$ (f) $\beta = 0.91,\ \omega = 0.77$

Figure 11. Dynamic perspective of the solution of (4.80) with the parameters $\mathscr{Q} = 2,\ B(t) = 0.7,\ \mathscr{M} = 0.62,\ \lambda_0 = 1.5$, and $\alpha = 0.9$.

7. Conclusions

In this study, we successfully studied the fractional stochastic KMMS as it relates to ferromagnetic materials, achieving analytical solutions by using the improved $\mathscr{F}$-expansion technique and the NEDAM. Through our investigation, we identified a variety of unique solutions, encompassing dark, dark–bright, bright–dark, singular, periodic, mixed trigonometric, and rational configurations. We used Mathematica to create three-dimensional, two-dimensional, density, and contour graphs using carefully chosen parameter values in order to highlight the physical relevance of the suggested model. The results illustrated how these techniques may effectively capture the fundamental properties of fractional stochastic equations by revealing the complex structures and dynamic behaviors of the system. Furthermore, a sensitivity analysis of the selected model has been conducted, offering important insights into the ways in which different parameters affect the system. It is expected that the knowledge gathered from this research will contribute to the creation of more accurate and efficient models for ferromagnetic materials, with potential applications in other fields needing exact analytical solutions to nonlinear fractional systems. To sum up, it is expected that experimental findings will support the theoretical frameworks found in this investigation. For example, if the relevant conditions are met, experimental studies of ferromagnetic materials may reveal soliton profiles like mixed trigonometric structures, periodic patterns, or dark and bright solitons. Through promoting a collaboration between theoretical forecasts and experimental verification, this study establishes a basis for furthering the comprehension and utilization of fractional stochastic systems in practical situations.

Use of Generative-AI tools declaration

The author declares that he has not used Artificial Intelligence (AI) tools in the creation of this article.

Acknowledgments

Researchers Supporting Project number (RSPD2025R526), King Saud University, Riyadh, Saudi Arabia.

Conflict of interest

The author declares that he has no conflict of interest.

Funding

Researchers Supporting Project number (RSPD2025R526), King Saud University, Riyadh, Saudi Arabia.

References

1. J. Liu, Z. Li, Bifurcation analysis and soliton solutions to the Kuralay equation via dynamic system analysis method and complete discrimination system method, *Qual. Theory Dyn. Syst.*, **23** (2024), 126. https://doi.org/10.1007/s12346-024-00990-5
2. M. A. El-Shorbagy, S. Akram, M. U. Rahman, Propagation of solitary wave solutions to (4+1)-dimensional Davey-Stewartson-Kadomtsev-Petviashvili equation arise in mathematical physics and stability analysis, *Partial Differ. Equ. Appl. Math.*, **10** (2024), 100669. https://doi.org/10.1016/j.padiff.2024.100669
3. M. U. Rahman, M. Sun, S. Boulaaras, D. Baleanu, Bifurcations, chaotic behavior, sensitivity analysis, and various soliton solutions for the extended nonlinear Schrödinger equation, *Bound. Value Probl.*, **2024** (2024), 15. https://doi.org/10.1186/s13661-024-01825-7
4. I. Alazman, B. S. T. Alkahtani, M. U. Rahman, M. N. Mishra, Nonlinear complex dynamical analysis and solitary waves for the (3+1)-D nonlinear extended quantum Zakharov-Kuznetsov equation, *Results Phys.*, **58** (2024), 107432. https://doi.org/10.1016/j.rinp.2024.107432
5. W. X. Qiu, Z. Z. Si, D. S. Mou, C. Q. Dai, J. T. Li, W. Liu, Data-driven vector degenerate and nondegenerate solitons of coupled nonlocal nonlinear Schrödinger equation via improved PINN algorithm, *Nonlinear Dyn.*, **113** (2025), 4063–4076. https://doi.org/10.1007/s11071-024-09648-y
6. Y. Q. Chen, Y. H. Tang, J. Manafian, H. Rezazadeh, M. S. Osman, Dark wave, rogue wave and perturbation solutions of Ivancevic option pricing model, *Nonlinear Dyn.*, **105** (2021), 2539–2548. https://doi.org/10.1007/s11071-021-06642-6
7. B. Li, Y. Zhang, X. Li, Z. Eskandari, Q. He, Bifurcation analysis and complex dynamics of a Kopel triopoly model, *J. Comput. Appl. Math.*, **426** (2023), 115089. https://doi.org/10.1016/j.cam.2023.115089
8. Z. Eskandari, Z. Avazzadeh, R. Khoshsiar Ghaziani, B. Li, Dynamics and bifurcations of a discrete-time Lotka-Volterra model using nonstandard finite difference discretization method, *Math. Meth. Appl. Sci.*, **48** (2025), 7197–7212. https://doi.org/10.1002/mma.8859
9. X. Zhu, P. Xia, Q. He, Z. Ni, L. Ni, Ensemble classifier design based on perturbation binary salp swarm algorithm for classification, *Comput. Model. Eng. Sci.*, **135** (2022), 653–671. https://doi.org/10.32604/cmes.2022.022985
10. Q. He, P. Xia, C. Hu, B. Li, Public information, actual intervention, and inflation expectations, *Transform. Bus. Econ.*, **21** (2022), 644–666.
11. R. Luo, Rafiullah, H. Emadifar, M. U. Rahman, Bifurcations, chaotic dynamics, sensitivity analysis and some novel optical solitons of the perturbed non-linear Schrödinger equation with Kerr law non-linearity, *Results Phys.*, **54** (2023), 107133. https://doi.org/10.1016/j.rinp.2023.107133
12. G. H. Tipu, W. A. Faridi, Z. Myrzakulova, R. Myrzakulov, S. A. AlQahtani, N. F. AlQahtani, et al., On optical soliton wave solutions of non-linear Kairat-X equation via new extended direct algebraic method, *Opt. Quant. Electron.*, **56** (2024), 655. https://doi.org/10.1007/s11082-024-06369-9
13. A. M. Talafha, A. Jhangeer, S. S. Kazmi, Dynamical analysis of (4+1)-dimensional Davey Srewartson Kadomtsev Petviashvili equation by employing Lie symmetry approach, *Ain Shams Eng. J.*, **14** (2023), 102537. https://doi.org/10.1016/j.asej.2023.102537

14. A. M. Alqahtani, S. Akram, J. Ahmad, K. A. Aldwoah, M. U. Rahman, Stochastic wave solutions of fractional Radhakrishnan-Kundu-Lakshmanan equation arising in optical fibers with their sensitivity analysis, *J. Opt.*, 2024. https://doi.org/10.1007/s12596-024-01850-w

15. A. Farooq, M. I. Khan, K. S. Nisar, N. A. Shah, A detailed analysis of the improved modified Korteweg-de Vries equation via the Jacobi elliptic function expansion method and the application of truncated M-fractional derivatives, *Results Phys.*, **59** (2024), 107604. https://doi.org/10.1016/j.rinp.2024.107604

16. H. Yépez-Martínez, M. S. Hashemi, A. S. Alshomrani, M. Inc, Analytical solutions for nonlinear systems using Nucci's reduction approach and generalized projective Riccati equations, *AIMS Mathematics*, **8** (2023), 16655–16690. https://doi.org/10.3934/math.2023852

17. S. Khajir, Z. Karimzadeh, M. Khoubnasabjafari, V. Jouyban-Gharamaleki, E. Rahimpour, A. Jouyban, A Rayleigh light scattering technique based on β-cyclodextrin modified gold nanoparticles for phenytoin determination in exhaled breath condensate, *J. Pharm. Biomed. Anal.*, **223** (2023), 115141. https://doi.org/10.1016/j.jpba.2022.115141

18. T. Yin, Z. Xing, J. Pang, Modified Hirota bilinear method to (3+1)-D variable coefficients generalized shallow water wave equation, *Nonlinear Dyn.*, **111** (2023), 9741–9752. https://doi.org/10.1007/s11071-023-08356-3

19. S. Naowarat, S. Saifullah, S. Ahmad, M. De la Sen, Periodic, singular and dark solitons of a generalized geophysical KdV equation by using the tanh-coth method, *Symmetry*, **15** (2023), 135. https://doi.org/10.3390/sym15010135

20. S. Tomar, M. Singh, K. Vajravelu, H. Ramos, Simplifying the variational iteration method: A new approach to obtain the Lagrange multiplier, *Math. Comput. Simulat.*, **204** (2023), 640–644. https://doi.org/10.1016/j.matcom.2022.09.003

21. J. Ahmad, S. Akram, K. Noor, M. Nadeem, A. Bucur, Y. Alsayaad, Soliton solutions of fractional extended nonlinear Schrödinger equation arising in plasma physics and nonlinear optical fiber, *Sci. Rep.*, **13** (2023), 10877. https://doi.org/10.1038/s41598-023-37757-y

22. M. T. Islam, T. Rahman, M. Inc, M. A. Akbar, Comprehensive soliton solutions of fractional stochastic Kraenkel-Manna-Merle equations in ferromagnetic materials, *Opt. Quant. Electron.*, **56** (2024), 927. https://doi.org/10.1007/s11082-024-06471-y

23. F. M. Al-Askar, The solitary wave solutions of the stochastic Heisenberg ferromagnetic spin chain equation using two different analytical methods, *Front. Phys.*, **11** (2023), 1267673. https://doi.org/10.3389/fphy.2023.1267673

24. M. A. E. Abdelrahman, M. A. Sohaly, Y. F. Alharbi, The new structure of stochastic solutions for the Heisenberg ferromagnetic spin chain equation, *Opt. Quant. Electron.*, **55** (2023), 694. https://doi.org/10.1007/s11082-023-04923-5

25. W. W. Mohammed, M. El-Morshedy, C. Cesarano, F. M. Al-Askar, Soliton solutions of fractional stochastic Kraenkel-Manna-Merle equations in ferromagnetic materials, *Fractal Fract.*, **7** (2023), 328. https://doi.org/10.3390/fractalfract7040328

26. S. Zhao, Z. Li, The analysis of traveling wave solutions and dynamical behavior for the stochastic coupled Maccari's system via Brownian motion, *Ain Shams Eng. J.*, **15** (2024), 103037. https://doi.org/10.1016/j.asej.2024.103037

27. Z. Li, J. Lyu, E. Hussain, Bifurcation, chaotic behaviors and solitary wave solutions for the fractional Twin-Core couplers with Kerr law non-linearity, *Sci. Rep.*, **14** (2024), 22616. https://doi.org/10.1038/s41598-024-74044-w

28. B. Q. Li, Y. L. Ma, Loop-like periodic waves and solitons to the Kraenkel-Manna-Merle system in ferrites, *J. Electromagn. Waves Appl.*, **32** (2018), 1275–1286. https://doi.org/10.1080/09205071.2018.1431156

29. B. Q. Li, Y. L. Ma, Rich soliton structures for the Kraenkel-Manna-Merle (KMM) system in ferromagnetic materials, *J. Supercond. Nov. Magn.*, **31** (2018), 1773–1778. https://doi.org/10.1007/s10948-017-4406-9

30. H. T. Tchokouansi, V. K. Kuetche, T. C. Kofane, On the propagation of solitons in ferrites: The inverse scattering approach, *Chaos Soliton Fract.*, **86** (2016), 64–74. https://doi.org/10.1016/j.chaos.2016.02.032

31. F. T. Nguepjouo, V. K. Kuetche, T. C. Kofane, Soliton interactions between multivalued localized waveguide channels within ferrites, *Phys. Rev. E*, **89** (2014), 063201. https://doi.org/10.1103/PhysRevE.89.063201

32. S. Saini, R. Kumar, Deeksha, R. Arora, K. Kumar, Symmetry analysis and wave solutions of the fisher equation using conformal fractional derivatives, *J. Appl. Math.*, **2023** (2023), 1633450. https://doi.org/10.1155/2023/1633450

33. A. Hussain, H. Ali, F. Zaman, N. Abbas, New closed form solutions of some nonlinear pseudo-parabolic models via a new extended direct algebraic method, *Int. J. Math. Comput. Eng.*, **2** (2023), 35–58. https://doi.org/10.2478/IJMCE-2024-0004

34. M. A. El-Shorbagy, S. Akram, M. U. Rahman, H. A. Nabwey, Analysis of bifurcation, chaotic structures, lump and $M-W$-shape soliton solutions to (2+1) complex modified Korteweg-de-Vries system, *AIMS Mathematics*, **9** (2024), 16116–16145. https://doi.org/10.3934/math.2024780

AIMS Press